Catalysis Science & Technology

Advances in Catalytic Production Processes of Bio-Derived Vinyl Monomers

Journal:	*Catalysis Science & Technology*
Manuscript ID	CY-MRV-03-2020-000598.R2
Article Type:	Minireview
Date Submitted by the Author:	28-Jun-2020
Complete List of Authors:	Avasthi, Kalpana; National Institute of Chemistry Slovenia, Department of Catalysis and Chemical Reaction Engineering Bohre, Ashish; Kemijski institut, Department of Catalysis and Chemical Reaction Engineering Grilc, Miha; National Institute of Chemistry, Department of Catalysis and Chemical Reaction Engineering Likozar, Blaž; National Institute of Chemistry, Department of Catalysis and Chemical Reaction Engineering Saha, Basudeb; University of Delaware, Catalysis Center for Energy Innovation;

Advances in Catalytic Production Processes of Bio-Derived Vinyl Monomers

Kalpana Avasthi, [a#] Ashish Bohre, [a# *] Miha Grilc,[a] Blaž Likozar, [a*] Basudeb Saha[b,c*]

[a]*Department of Catalysis and Chemical Reaction Engineering, National Institute of Chemistry, Hajdrihova 19, 1000 Ljubljana, Slovenia*

[b]*Catalysis Center for Energy Innovation, University of Delaware, Newark, DE 19716, USA*

[c]*RiKarbon, Inc., 550 S. College Ave, Newark, Delaware, DE 19716, USA.*

[#]Equal contribution

*Corresponding author's *E-mail addresses:* bsaha@udel.edu, bsaha@rikarbon.com
blaz.likozar@ki.si, ashish.bohre@ki.si

ABSTRACT

Plastics industry technologies currently source the majority of monomers from crude oil substances. Although we have witnessed a significant companies' interest towards the utilization of the sustainable feedstock materials for the bio-based compound synthesis in a the past decade, the transition to the photosynthetic or chemosynthetic plant-based production in a circular carbon economy is largely slow due to complex biomass processing, costs and related reaction factors. The upgrade of the separated platform chemicals with a deeper supporting understanding of processes, models and a root cause analysis about the underlying distribution challenges of engineered transformation mechanisms, catalyzed conversion pathways and selectivity would be beneficial to advance applied scientific development, bio-refining and manufacturing output amount. This review provides a summary, assessment and perspective for three important polymer-forming vinyl molecules, *i.e.* acrylic acid, methacrylic acid and styrene. These provide a backbone to produce acrylates, polystyrene, resins, rubbers, protective surface coatings, adhesives, textiles and other obtained copolymers. A succinct analytical overview on the thermo-catalytic intermediate routes for property-wise drop-in alternatives is presented. Sugars, acrolein, allyl alcohol, ethylbenzene, glycerol, 3-hydroxypropionic acid, isobutene, itaconic acid and lactic acid are considered as main starting reactants. Catalysts span mixed metal oxides, silicates, native or impregnated zeolite frameworks (HBEA, HZSM, and MFI) and hetero-poly acids as well as homogeneous base hydroxides or platinum group metals, supported on carbon, alumina and sulfates. The article concludes with a brief state sum-up of the results, topics and opportunities for systematic future research or scaling.

Keywords:

Bio-based monomer, Heterogeneous catalyst, Acrylic acid, Methacrylic acid, Styrene, Biomass feedstock

• Introduction

The Polymeric materials play a vital role in modern society, occupying an ever-expanding range of uses from the materials that are used in automobiles and textile sectors to those with sophisticated applications in medical science and electronics.[1] The global plastics production has reached 359 million tonnes in 2018, which is expected to double by 2035.[2] The majority of plastics produced by the polymer industries are derived from fossil sources. The gap between the supply and demand of fuels and chemicals have increased due to the increasing population growth rate and finite nature of fossil resource.[3] Non-renewable fossil sources meets nearly 86% of the world's energy and 96% of basic, commodity and specialty chemical demands.[4] Depletion of these sources, rising socio-economic and environmental concerns require a reduction of our dependence on the eventually depleting conventional sources of energy.[5]

In order to make polymer industries sustainable, a carbon neutral feedstock with an abundant supply is a promising alternative.[6] Bio-based monomers play a critical role to this sustainable initiative.[7] The bio-based plastics industry is still in its infancy and growing fast, due to consumer's pressure for renewable products, global environmental challenges and concerns about depleted petroleum resources. The production of bio-based polymer from renewable resources is an emerging research and commercial focus. Naturally occurring polymers, such as lignocellulose sourced from forest, agricultural residues, municipal waste, can be either used as a polymer backbones or deconstructed into platform chemicals, and can serve as a promising feedstock to produce bio-based monomers and polymers to improve future energy security and mitigate environmental challenges.[8-9]

Upgrade of lignocellulosic biomass to bio-based monomers for polymer production involves two main strategies *i.e.* bio-polymer strategy and drop-in strategy.[10] In the bio-polymer strategy, new biomass derived polymers are synthesized by adopting chemical and biological transformation routes while in the drop-in strategy, existing monomers, derived from petroleum, are produced from biomass.[11]

The bio-polymer approach brings new product offering and new market opportunities to the chemical industry; however it requires an extensive development time and high capital investment. In contrast, the drop-in approach produces products that are already in use and have established markets and supply chains, e.g., bioethylene and biopropylene.[12-14]

Vinyl monomers are industrially important commodity chemicals, which are widely used to produce polyacrylate, polystyrene, adhesives, protective coatings, resins, rubbers and other copolymers.[15] The chemical structure of vinyl monomers contain an active double bond that can be further functionalized to yield versatile synthetic intermediates and polymers. In this review, recent catalytic transformation strategies employed to produce three important vinyl monomers - acrylic acid (AA), methacrylic acid (MAA) and styrene (ST) are discussed. The precursors of these monomers, such as itaconic acid, glycerol, allyl alcohol, lactic acid, acrolein (Fig. 1) can be derived from biomass.[16]

(Figure 1 here)

Scope of this review

Significant research endeavors have been undertaken towards developing sustainable polymers in the past decade.[17] This initiative resulted in publication of several review articles. For example, Shiju *et al.* provided a critical overview on the transformation from fossil-based to bio-based production of acrylic acid, adipic acid and ε-caprolactam.[18] Williams *et al.* described a sustainable strategy for the production of polymers from carbon dioxide, terpenes, vegetable oils and carbohydrates.[8] In 2016, Palkovits *et al.* has published a comprehensive review on the production of bio-based monomers and their application for polymer production.[19] Ferrario *et al.* has provided an overview on the production of renewable polyesters by biotechnological routes.[20] Sels and co-authors have discussed the catalytic advancements in the bio-based polyester monomers from carbohydrates.[21] Loos *et al.* reported a critical review, focusing on recent development in chemical modifications of bio-based polymers and building blocks for new polymers.[22] In 2019, the Lee group published a critical review on polymers derived from hemicellulosic building blocks (furfural) of lignocellulosic biomass.[23] Huang *et al*. summarized the recent development of stimuli-responsive renewable polymeric materials and their applications.[24] The production of lower olefins such as ethylene, propylene, and butylenes from biomass derived feedstocks has been comprehensively reviewed.[25] A few reviews described the environmental, social and economic impact of bio-based monomers and polymers.[26] Several review articles on sustainable production of AA or

MAA or ST have been reported. Makshina *et al.* reported the production of AA by using lactic acid and their derivatives.[27]

Patience and co-workers discussed the roles of catalysts for the production of MAA and methyl methacrylate (MMA).[28] Nagaraja *et al.* presented several aspects of the oxidative dehydrogenation of ethylbenzene to ST with vanadium, iron, mixed oxide and carbon based catalysts.[29]

Although these reviews provide useful implications and insights, none of them sheds light on the detailed sustainable production routes of these vinyl monomers. Hence, a timely comprehensive review, highlighting the recent progress in catalytic and biotransformation routes of these monomers from renewable feedstocks is essential to benefit both academia and industry researchers. Therefore, the major objective of this review is to present a concise summary on the economically viable and environmentally benign processes and feedstocks diversity to produce aforementioned three monomers. Another objective is to provide an outlook and future research directions. This review article is not intended to describe the Life cycle and techno-economic analyses.

The content of this article has been divided into sections as summarized in the table of content. First, an overview of the aforementioned three vinyl monomers, and their industrial production processes is introduced. Next, the global market and application landscape are presented. The discussion followed with a brief review on several promising conversion approaches and renewable feedstocks development. Finally, a brief summary on the challenges and opportunities of future research is presented. We believe this comprehensive review will serve as a stepping-stone to new efforts towards developing sustainable routes for the production of bio-based monomers.

- **Acrylic acid (AA)**

AA is a versatile monomer and intermediate for the manufacture of various industrial and consumer products.[27] AA and its esters are the top 25th organic chemical products with annual production capacity of about 6 million tons[30] and growth rate of 5.14% per year.[31] AA Market size was about $11,006 million in 2013 and is expected to reach $18,824 million by 2020.[32] According to global opportunity analysis and industry forecast, global consumption of AA is expected to reach 8,169 kilotons by 2020.[33] Important characteristics of acrylate polymers such as faded transparency, facile adhesion, elasticity, stability under light and average heat make them suitable candidate for the manufacture of paints and coatings materials.[34]

Conventionally AA is produced via oxidation of fossil-based propylene at high temperature. Industrially, AA is produced via two-step fossil-based propylene oxidation process in fixed-bed tubular reactor over molybdenum-based heterogeneous catalyst.[35] Because of reliance on fossil fuels and petroleum-based AA contributes to harmful greenhouse gas emission,[36] utilization of bio-based feedstocks such as lactic acid, acrolein, glycerol, 3-hydroxypropionic acid (Fig. 2) to produce AA is increasing. In the following sections, we will describe different types of bio-based materials and methods for the production of AA.

(Figure 2 here)

AA production from different bio-based feedstocks

Glycerol to AA. Presently, glycerol is produced as a byproduct of biodiesel through *trans*-esterification of vegetable oils.[37] Remarkable growth in the biodiesel industries in recent years has led to an increased production of crude glycerol that can be converted to value added chemicals through chemical and biological routes.[38-39] Typically, 100 kg of biodiesel yields 10 kg of glycerol.[40] The synthesis of AA from glycerol involves single and two step approaches as shown in Scheme 1. In the two-step approach, AA can be prepared through acrolein and allyl alcohol intermediates, respectively.[41] For industrial production, one step process is beneficial. In the single step production of AA, the dehydrogenation of glycerol to acrolein and oxidation of acrolein to AA take place over a single multifunctional catalyst bed using O_2 or air as an oxidant. Several catalysts having acidic and redox sites have been reported for the one-step oxidative dehydrogenation of glycerol to AA.

Table 1 summarizes the results from vapor-phase oxidative dehydration of glycerol.

(Scheme 1 here)

(Table 1 here)

Chieregato *et al*. developed W-Nb-O and W-Nb-V-O mixed oxides catalysts and tested their activity for oxidative transformation of glycerol to AA (Table 1, entry 1).[42] The authors have achieved 34% AA yield over the W-V-Nb-O bronze catalyst. Acrolein was formed (17%) as a side product due to the dehydration of glycerol. It was proposed that W-Nb-O promotes the dehydration of glycerol to acrolein, while V sites catalyze the oxidation of acrolein. In 2010, Ueda *et al.* developed an embedded catalyst in which iron oxide domains impregnated on the surface of an iron orthovanadate ($FeVO_4$) phase.[243] The proximity of the two phases promoted the dehydration and oxidation in a single step that resulted in 14% AA yield (Table 1, entry 2). Later, it was found that the addition of W in place of Fe improved the yield

of AA up to 26% (Table 1, entry 3). [244] In 2014, Nieto *et al.* reported that the incorporation of Nb with W and V enhanced the number of acidic sites required for the dehydration reaction, which resulted in 51 % AA selectivity (Table 1, entry 4). [245] It was also claimed in a few reports that the addition of Mo with W–V mixed oxide changes the Brønsted acid and redox sites. However, AA selectivity remained below 43% (Table 1, entry 5-6). [246 247] In 2016, Ueda *et al.* modified the surface of the W-V-Nb-O bronze catalyst with phosphorus oxide, which showed an improvement in the yield of AA (60%) (Table 1, entry 7).[43] The incorporation of phosphorus oxide in W-V-Nb-O structure generated strong acid sites.

Heteropoly acids have strong Brønsted acid sites.[44] Thanasilp *et al*. performed the oxidation of glycerol over Al_2O_3-supported heteropoly acids and V-modified $H_3SiW_{12}O_{40}$/HZSM-5 catalysts. The highest AA yield of 36% was obtained over $VH_3SiW_{12}O_{40}$/HZSM-5 in 6 h at 90 °C (Table 1, entry 8).[45] Inspired by this work, Zhang *et al.* studied the dehydration of glycerol to AA in a single reactor using Keggin-type heteropoly acids in 2016.[46] They tested several cesium salts supported heteropoly acids and found that $H_{0.1}Cs_{2.5}(VO)_{0.2}PW_{12}O_{40}$ was an effective (60% yield) and stable catalyst to produce AA from glycerol (Table 1, entry 9).

The modification of acidic zeolites using oxidation sites such as V and Fe was attempted by several groups.[47-48] However, the modified catalysts were not active and high amount of side products such as acetaldehyde and acetic acid were obtained (Table 1, entry 10). It was observed that low acidity and high oxidation ability are two important factors to achieve high yield of AA. Sarkar *et al.* prepared a Cu/SiO_2-MnO_2 catalyst and achieved 74% selectivity to AA with glycerol conversion of 77% at 70 °C for 30 h. It was found that dehydration of glycerol to acrolein was promoted by the acid sites of SiO_2-MnO_2, whereas the presence of Cu^+ sites oxidized acrolein to AA (Table 1, entry 11).[49]

Zeolites are rarely used for oxidative dehydrogenation of glycerol. However, the incorporation of oxidation spices such as V, W Mo or Fe can improve the catalytic activity of zeolites. Diallo *et al.* demonstrated that the catalytic activity of BEA zeolites can be improved by the addition of Fe(III) tetrahedral species. The selectivity to AA was 26% at glycerol conversion of >99% at 275 °C (Table 1, entry 12).[50] Most recently, Mascarenhas *et al.* developed a bifunctional H,Fe-MCM-22 catalyst for the gas-phase oxidative dehydrogenation of glycerol.[51] AA yield improved with processing time, reaching 57% at 320 °C after 10 h over the catalyst containing 1.2 wt.% of iron (Table 1, entry 13). HZSM-5 is known have high surface area and stability at high temperature. When MVO mixed oxide was impregnated on

HZSM-5, maximum 47% AA selectivity was achieved at 250 °C (Table 1, entry 14). [247] The yield was slightly lower at higher temperature (300 °C) as reported by Sooknoi *et al.* (Table 1, entry 15).[251]

Lactic acid (LA) to AA. LA is the most widely occurring carboxylic acid in nature and is currently produced by fermentation of glucose and sucrose.[52] The global production of LA is about 367,000 tons per year and is estimated to have substantial growth in the next decade. The catalytic dehydration of LA to AA is a promising but challenging route. Several parallel reactions such as decarbonylation and decarboxylation compete with the dehydration of LA that inhibits the overall AA yield. Varieties of catalysts with different active sites have been tested for this reaction. In order to better identify the recent catalytic advancements and developments, we have divided the catalysts into three groups: *i.e.* zeolites, phosphates and sulphates, and they are discussed below.

Owning to the large surface area and well-balanced acid-base sites, zeolites are most frequently investigated heterogeneous catalysts for AA formation from LA. Among the different tested zeolites, NaY zeolite has extensively studied. NaY is a class of zeolite belongs to Faujasite (FAU) family, has Si/Al molar ratio above 1.5.[53] It was reported that unmodified NaY zeolite is less active for the production of AA. To enhance the activity, Lari *et al.* prepared NaY zeolite with different Si/Al ratios. It was observed that the high Si/Al ratio favours the formation of acetaldehyde as a side product that decrees the yield of AA. Similar results were obtained by other researchers, confirming that structural modification is essential to increase AA selectivity.[54-55]

To improve the activity of NaY zeolite, different alkali phosphates, rare earth metals (La, Ce, Sm, and Eu) and mixed oxides were doped with parent NaY. [56-57] Such modifications have shown improved catalytic performances due to the tuned acidity/basicity and metal electronic promoter effect of dopant that enhance the adsorption of substrate/product and reduce the formation of side-products.[58] When we compared the activity of individual dopant, potassium modified NaY zeolites exhibited better catalytic performance. In two separate studies, Huang *et al*. modified the NaY zeolites by potassium and alkaline earth metals and tested for LA dehydration under similar reaction conditions.[59-60] They found that the impregnation of potassium in the catalyst had a positive effect on the AA selectivity. The best result (68% selectivity) was obtained over NaY zeolite modified with KI (3.3 wt.% of K loading). The detailed structural investigation implies that doping of potassium reduced the strength and density of zeolite acid sites and improves AA selectivity. Another research group

co-modified NaY zeolite with alkali and alkaline-earth metal.[61] The high AA selectivity of about 84% and complete conversion of LA were reported with KOH Ca/NaY catalyst. After four regeneration cycles the catalyst exhibited good stability produces AA with 82% selectivity. According to the authors, stepwise modifications of the zeolite surface first with calcium nitrate and then with KOH significantly reduce the acidic and basic site that led to enhance AA selectivity. The best results (99% yield) till date for the production of AA was patented by Zuo *et al.* using mixed Li-montmorillonite-NaY catalyst.[62] However, the active sites of the catalyst responsible for such a remarkable performance have not disclosed.

Despite promising results, many authors reported the deactivation of the catalyst during the course of the reaction by coke formation. Näfe *et al.* identified that the deposition of lactic acid and its open-chain esters on the surface deactivate the catalyst.[55] To tackle this issue, larger cations such as K and Cs were impregnated with NaY zeolite to block the pores. In case of alkaline metal doped NaY zeolites, lattice polarity and adsorption capacity are the important factors that affect the deactivation of the catalyst.[55] It was also reported that the nanocrystallites NaY zeolites are more stable and active compared to commercial NaY zeolites. Ji *et al*. prepared NaY zeolites of different particle sizes by regulating the H_2O/SiO_2 molar ratio and doped with Na_2HPO_4.[58] The catalyst with the lowest particle size of NaY (20 nm) with 12 wt.% loading of Na_2HPO_4 yielded 74.3% AA at 340 °C. The catalyst is structurally stable and doesn't lose activity after four consecutive cycles as confirmed by the XRD investigation. The excellent catalytic activity was explained by appropriate surface acidity together with unique structural features of the catalyst.

Zeolite β (BEA) is another class of zeolite that has been widely used for AA synthesis from LA due to its porous structure and easily tuneable acid-base and redox properties.[63] Similar to NaY, unmodified β zeolite rarely catalyse the dehydration of LA to AA. Thus, metal-ion exchanged forms of zeolite β have frequently been used to improve their catalytic properties. Different research groups have achieved better AA selectivity and yield from Li, K, Rb and Cs ion-exchanged β zeolites compared to bare β zeolite.[63-64] Yan *et al.* observed that the catalytic activity of alkali-exchanged β zeolite was significantly affected by the type of counter ion.[64] Alkali-exchanged β zeolite prepared from potassium, rubidium and cesium exhibited better catalytic performance (64 mol% AA selectivity) while sodium and lithium promote side reactions. This catalytic behavior was explained by the presence of balanced surface acidity and basicity of ion-exchanged β zeolites that enable high AA selectivity.

Besides β zeolite and NaY, ZSM-5 zeolite was also studied by few groups.[65] Zhang *et al.* modified HZSM-5 by treatments of NaOH and Na_2HPO_4 and tested for dehydration of LA

to AA.[66] Excellent AA selectivity (78%) and high LA conversion was achieved over the modified ZSM-5 catalyst. The modification induced some extra mesopores, resulting in large number of medium acidic and basic sites. The impregnation of sodium or potassium phosphate salt further improved the activity of alkali treated ZSM-5 zeolite.[66-68]

The bulk phosphate catalysts have gained momentum for the production of AA.[69] Among the different phosphate materials, calcium hydroxyapatite (HAP) has gained a particular interest.[70-72] In HAP catalysts, weak and moderate acid/base sites promote LA dehydration, whereas strong acid/base side preferred side reactions such as decarbonylation and decarboxylation. The excellent catalytic activity of HAP is associated with the balanced acidic and basic sites that can be obtained by the tuning of Ca/P ratio. This is achieved by controlling the pH of the synthetic solution by using ammonia gas, aqueous ammonia or alkaline hydroxide.[73] Processing temperature is another factor that affects the activity of HAP because high calcination temperature reduces the surface area of the catalyst, results in less number of active sites to promote dehydration.

When the activity of HAP is correlated on the basis of Ca/P ratio, an exact trend was unclear because different authors have used different reaction conditions. For instance, Ghantani *et al.* prepared a series of HAP catalysts by changing the Ca/P ratio ranging from 1.3 to 1.89. It was observed that the decreasing Ca/P ratio produced more AA. They achieved 60% selectivity of AA at the complete conversion of LA at 375 °C with a Ca/P ratio of 1.3 (Scheme 2).[70] Xu *et al.* found contrasting behavior of Ca/P ratio on AA selectivity.[74] They reported an increase in AA selectivity with an increase of Ca/P ratio and achieved 71-74 mol% AA selectivity at a Ca/P ratio of 1.62. This volcano-type correlation between Ca/P ratio and AA selectivity was explained by the ratio of acid to basic sites.

(Scheme 2 here)

Similar to Ca/P ratio, the catalytic activity can also be improved by introducing alkali salts within the framework of HAP. Dongare *et al.* claimed that the modification of HAP with trisodium phosphate ($Na_3PO_4 \cdot 12H_2O$) resulted in an enhanced AA selectivity up to 70% with a complete conversion of LA.[75] In another study, comparatively lower AA yield (60%) was obtained from disodium hydrogen phosphate and sodium nitrate precursors.[70] In contrast, post-synthetic impregnation of Ca-HAP with NaOH or KOH showed relatively low AA yield (32%) and high selectivity to acetaldehyde and 2,3-pentanedione by-products.[72] This is most probably due to the high basicity of the catalyst that promotes the side reactions.[76]

Besides HAP materials (HAPs), alkali earth metal pyrophosphates (MPP) and orthophosphates (MOP) have also been studied.[73, 77-79] Ghantani *et al.* reported that the yield of AA significantly depends upon the Ca/P ratio for calcium pyrophosphate catalysed LA dehydration reaction.[77] They achieved 78% AA selectivity with complete conversion of LA at low Ca/P ratio of 0.76. In contrast, low AA selectivity (50%) was obtained at a high Ca/P ratio.[73] The high AA selectivity was obtained due to the increased acidity and reduced basicity of the catalyst.

Similar to HAPs, several dopants have been proposed to further improve the catalytic activities of MPP and MOP materials. For instance, calcium orthophosphate doping with K_2HPO_4 by pre-synthetic modification procedure resulted in unprecedentedly high AA selectivity of 93% at 91% LA conversion. However, the addition of K_2HPO_4 salt after precipitation (post-synthetic modification) significantly reduced the AA selectivity (42%).[80-81] Tang *et al.* found contrasting results when strontium pyrophosphate modified by phosphoric acid.[78] Under the optimized reaction conditions, phosphoric acid impregnated strontium pyrophosphate catalyst completely converted LA with 72% selectivity to AA selectivity. They also used weakly acidic dibarium pyrophosphate, which slightly improved the selectivity of AA (76%).[79]

In addition to the aforementioned alkaline-earth phosphate materials, the catalytic capabilities of lanthanum and cerium phosphate salts were also explored. In 2016, Guo *et al.* described a new approach for the production of AA from lanthanum phosphate (LaP) nano-rods.[82] The shape-directing agent (SDA), n-butylamine, improved the porosity of LaP materials as well as modified the acid/base properties. Their investigation reveals that Lewis acidity due to La^{3+} cations in LaP materials play an essential role in the catalytic dehydration of LA to AA, whereas basicity results in catalyst deactivation. The highest LA conversion (67%) and AA selectivity (50%) were achieved when using LaP-3 (SDA/La molar ratio 3) at 350 °C. Nagaraju *et al.* prepared a series of cerium phosphate (CP) catalysts by changing the Ce/P mole ratios ranging from 0.5 to 3.0 and tested for LA dehydration under vapor-phase reaction conditions.[83] Among the CP catalyst, the catalyst with Ce/P mole ratio of 2.5 (CeP-2.5) showed the highest AA selectivity (64%) with almost complete conversion of LA. They found that the catalytic performance strongly depends upon the ratio of acidic/basic sites on the catalyst surface.

Besides phosphates, sulphate salts have also emerged as interesting catalysts for the production of AA.[82-86] The catalytic performance of sulphate salts strongly correlated with their acid/base properties. Peng *et al.* tested the catalytic activity of different metal sulphates

for dehydration of LA to AA and revealed that Mg, Ca and Ba sulphates having moderate and weak acidity are effective for this reaction. Strongly acidic Al, Ni and Zn sulfates promoted the formation of acetaldehyde. Among Mg, Ca and Ba sulfates, $BaSO_4$ catalyst exhibited an excellent catalytic activity, producing AA with 74% selectivity at nearly complete conversion of LA. The effect of the catalyst calcination temperature on AA selectivity was also investigated. The catalyst calcined at high temperature (700 °C) produced more AA compared to one calcined at lower temperature (500 °C). This is due to the increased weak and moderate acid site density of the catalyst with calcination temperature.

Similar to phosphate salts, the catalytic activity of sulfates can also be improved by doping with other salts. For example, doping of $CaSO_4$ with Na_2SO_4 can produce 68% AA at 400 °C. However, under similar reaction conditions doping with $Na_2P_2O_7$ gave a low yield (51%) of AA.[69] Zhang *et al.* promoted $CaSO_4$ catalyst with $CuSO_4$, Na_2HPO_4 and KH_2PO_4 salts and obtained 64% AA yield at 330 °C.[85]Authors have also investigated the effects of carrier gas (CO_2) and catalyst calcination temperature on AA yield. It was observed that the dehydration of LA is very sensitive to catalyst calcination temperature. A significant drop in the activity was detected with the catalyst prepared at low calcination temperature. This might be due to the changes in the strength, distribution and density of the acid sites. The Vos group recently developed an interesting catalytic system in which ionic liquid (IL) tetrabutylphosphonium bromide acts as a catalytic solvent and as an acid site for the dehydration of LA to AA.[87] The yield of AA was up to 70% within 3 h after the addition of a small amount of inexpensive acid, H_2SO_4, as a co-catalyst.

Acrolein to AA. Bio-based acrolein is produced from glycerol. Acrolein is also an intermediate in the process of propylene oxidation to AA, although this process does not provide commercial acrolein.[88] The glycerol-acrolein-AA route has some advantages over propylene-AA route. The main advantage is the utilization of sustainable feedstock that can reduce our dependence to fossil feedstock. Corma *et al.* reported that the production of AA from glycerol dehydration is economically more beneficial compared to petroleum-based production.[89] Utilization of waste glycerol, obtained from biorefineries, can make bio-based AA production even more attractive economically. However, there are some technological barriers that rendered the commercialization of this process. The acrolein produce from waste glycerol contains impurities such as methanol, NaOH, and other salts that deactivate the catalyst and promotes the side reactions. The purification of the waste glycerol adds extra cost and makes the AA production process economically unachievable. Several catalysts have been proposed that can endure the impurities in crude glycerol.[89] In order to briefly describe

the most important findings, we have divided the catalysts in two groups *i.e.* vanadium-molybdenum catalysts and nanocarbon-based catalysts.

Vanadium-molybdenum catalysts. Microporous crystalline molybdenum-vanadium mixed oxides (MoVO) are promising catalysts for the selective oxidation of acrolein to AA.[90-93] MoVO catalysts are formed by assembling giant polyoxometalate unites under hydrothermal conditions.[94] The network arrangement of these catalysts composed of a $\{Mo_6O_{21}\}^{6-}$ pentagonal unit and a $\{MO_6\}$ (M = Mo, V) octahedral unit that forms hexagonal and heptagonal channels. It is possible to obtained 4 distinct crystalline MoVO materials (orthorhombic MoVO, trigonal MoVO, tetragonal MoVO and amorphous MoVO) by tuning the preparation conditions.

The activity of MoVO catalysts strongly depends upon crystal structure and microporosity. For instance, orthorhombic Mo_3VO_x catalyst prepared by decreasing the pH of precursor solution showed improved AA selectivity (94%) and complete conversion of acrolein, compared to trigonal and amorphous Mo_3VO_x catalysts, while tetragonal MoVO was inactive.[91] According to the N_2 adsorption analysis, the volume of micropore is higher in orthorhombic Mo_3VO_x catalyst (14.0 $cm^3\ g^{-1}$) than those of trigonal (4.0 $cm^3\ g^{-1}$) and amorphous (2.8 $cm^3\ g^{-1}$) Mo_3VO_x catalysts, while no microporosity was detected in tetragonal Mo_3VO_x catalyst. The orthorhombic Mo_3VO_x (Orth-MoVO) catalyst possesses more accessible active surface comprising a heptagonal channel with micropore of 0.40 nm in which small molecules like acrolein can be easily adsorbed.

In order to explain the important role of heptagonal channels in the selective oxidation of acrolein, several ortho-MoVO catalysts with the same micropore volumes, but different external surface areas were prepared by using anionic surfactant, sodium dodecyl sulphonate under temperature controlled hydrothermal method.[90] The authors found a linear relationship between external surface areas and AA selectivity. In all the experiments, the catalysts with high external surface areas are effective and selective than those with low external surface areas. This clearly indicates that the heptagonal channels on the external surface of the catalysts promote acrolein conversion.

Besides the crystal structure, Mo/V ratio is also decisive to AA selectivity. The exact Mo/V molar ratio necessary for optimum results varies based on the preparation conditions of the catalyst. Adams *et al.* prepared Mo-V catalyst from vanadium pentoxide and molybdenum trioxide precursors. Mo-V catalyst with Mo/V ratio of 0.42 was the most promising with respect to the selectivity and activity at low temperatures.[95] In contrast, when Mo-V catalyst was prepared hydrochemically and dried via crystallisation and spray drying, a relatively

higher Mo/V ratio of about 3 was found to be the most effective and selective.[96] Eichel *et al.* studied the $Mo_{1-x}V_xO_y$ solid-solution systems ($0 \leq x \leq 10$) by electron paramagnetic resonance (EPR) spectroscopy. [97] When vanadium oxide was added to molybdenum oxide, the activity of the catalyst significantly improved and a volcano-type dependence of AA selectivity on vanadium content (VO^{2+}) was observed. Alike to Mo-V catalyst, maximal performance is obtained for a Mo/V ratio of 3:1.

The oxidation of acrolein over pure Mo-V mixed oxide required high temperature and oxygen pressure that results in deactivation of the catalyst. [98- 99] However, a small addition of tungsten remarkably improved the performance and stability of the Mo-V mixed oxide catalysts. In the structure of Mo-V-W mixed oxides, corner-linked tungsten-oxygen octahedrons prevent the agglomeration of corner-linked metal-oxygen octahedrons and improve the stability.[100] It was noticed that similar to the oxides of molybdenum, pure WO_3 remains inert during this reaction.

The structure of Mo-V-W mixed oxides is sensitive to vanadium doping and also changes during the oxidation of acrolein to AA.[101] Several techniques such as electron paramagnetic resonance (EPR), X-ray diffraction (XRD), temperature programmed reduction (TPR), and X-ray absorption near edge structure spectroscopy (XANES) were applied to identify the structure and structural modifications of Mo-V-W mixed oxides.[102-105] Giebeler *et al.* prepared solid solutions of $Mo_8V_2W_xO_y$ ($0 \leq x \leq 5$) by spray drying and crystallization methods and their structural changes were examined by XRD and TPR. The structural changes of the samples were identified by the Rietveld refinements method. The samples prepared by the crystallization method contained only stable orthorhombic MoO_3 or MoV_2O_8 phases with low tungsten loading and $Mo_{0.6}W_{0.4}O_3$ and $Mo_{0.29}W_{0.71}O_3$ phases were identified with high tungsten content. A complete structural transformation was detected with low (MoO_2 or VO_2) and high tungsten loading for the samples prepared by spray drying method. In both samples, higher selectivity towards AA with increasing tungsten content was observed.

Thankamony *et al.* applied ^{51}V solid-state dynamic nuclear polarization NMR spectroscopy to characterize the surface species of Mo-V-W mixed oxide catalyst prepared by a hydrothermal synthesis route.[102] The authors prepared three samples ($Mo_8V_2W_{0.5}O_y$ $Mo_8V_2W_1O_y$ and $Mo_8V_2W_{1.5}O_y$) containing the same V/Mo ratios, but with different tungsten contents. $Mo_8V_2W_{0.5}O_y$ showed the best enhancement of surface near ^{51}V nuclei. The authors have also tested the influence of pH-value on the preparation of the catalysts. Low pH (0.1) was beneficial to obtain the catalyst with high surface area.

Besides the crystal structure and tungsten doping, water played a crucial role in Mo-V-W-mixed oxide catalysed acrolein oxidation reaction.[106] Jekewitz *et al.* investigated the influence of water on gas phase oxidation of acrolein to AA over Mo-V-W-mixed oxide catalyst by temperature-programmed reactions method.[107] It was observed that the addition of water speeds up acrolein oxidation especially at low temperature. The promotional effect of water was explained by the fact that adsorbs water on metal oxides surface formed hydroxyl groups that acts as additional active sites for acrolein oxidation. To further clarify the role of water, steady-state isotopic transient kinetic analysis experiments with $H_2{}^{18}O$ were conducted in the temperature range of 90-345 °C at ambient pressure.[108] It was noticed that the conversion of acrolein to AA increases by two times (from 27% to 68%) upon increasing the water concentration from 13 mol% to 25 mol%. In this process, oxygen originating from ^{18}O labelled water is found in acrolein even at very low temperature. These isotopic tracer experiments also indicate that water promotes AA formation during acrolein oxidation.

In addition to tungsten, Fe and Cu metals have also been successfully introduced within the framework of Mo-V mixed oxide.[109-112] The activity of such modified Mo-V metal oxides strongly depends upon the doped metals and local structure of dopant. For instance, introduction of Cu improved AA selectivity up to 98% from 93% obtained over the parent Mo-V mixed oxide.[110] In the structure of Mo-V-Cu mixed oxide, Cu is located at the heptagonal channels sites that make the activation of molecular oxygen moderate and prevent side reactions. In a comparative study, it was observed that the doping of Fe in trigonal Mo-V metal oxides catalyst produce more AA compared to Cu.[113]

Nanocarbon-based Catalysts. Nanocarbons are another class of materials have gained increasing attention for AA formation from acrolein. Several nanostructured carbon based catalysts have been proposed for acrolein oxidation, namely natural and synthetic graphite, multi-walled carbon nanotubes (MWCNTs), fishbone-type carbon nanofibers (CNF), onion-like carbon (OLC), nano-diamond, fullerenes and activated carbon.[114-115]Among them, MWCNTs was the most active, selective, and highly robust catalyst towards AA formation. A high AA yield of 85% at 14% acrolein conversion was demonstrated by MWCNTs at 300 °C. AA selectivity over other nanocarbon materials was low, ranging between 12% and 75%. It was assumed that the surface functional groups played a crucial role in this reaction.

In order to check this hypothesis, different oxidized carbon nanotubes (o-CNTs) were prepared by tuned the surface concentration of oxygen functional groups and employed for the selective oxidation of acrolein to AA.[116] The important role of epoxy and lactone groups to achieve better AA selectivity was clearly demonstrated in this study. The mechanistic study

showed that epoxy and lactone groups take parts in the activation and oxidation of acrolein. Through proper fine-tuning of epoxy and lactone groups, AA selectivity of 80% at 51% acrolein conversion was obtained.

The activity of functionalized CNTs is significantly affected by the presence of carbonaceous species. It is necessary to remove such impurities before functionalizing the surface of CNTs. Zhong *et al.* recently investigated the influence of graphitization and oxidation on the catalytic activity of the CNTs.[117] The results suggested that the removal of amorphous carbon by graphitization accelerate the formation rate of AA by promoting the adsorption and activation of acrolein.

3-Hydroxypropionic acid (3-HPA) to AA. 3-HPA is a promising versatile substance derived from renewable feedstocks glycerol and glucose.[118] The United States Department of Energy has listed 3-HPA as one of the top 12 value-added platform compounds among bio-based products. Dehydration of 3-HPA and thermolysis of poly(3-Hydroxypropionate) are two approaches presently utilized to prepare AA. Dehydration of 3-HPA over an acidic catalyst is a viable route to produce AA.[119] Craciun *et al.* patented a novel method to produce AA by using high surface area γ-alumina, silica and TiO_2 (anatase) catalysts. Among them, γ-alumina and silica catalysts yielded above 97% AA in a gas phase fixed-bed reactor at 250 °C, whereas TiO_2 exhibited relatively low catalytic performance .[120] In contrast to this work, other patents claimed excellent performance of TiO_2 (anatase) catalyst with an AA selectivity of 99% and complete conversion of 3-HPA at 180-230 °C.[121-122] Similarly, Dishisha and co-workers proposed a two-step biochemical transformation to AA from glycerol. Resting cells of *Lactobacillus reuteri* was utilized as a biocatalyst to produce 3-HPA from glycerol in a fed-batch mode. In the second step, the solution of 3-HPA was dehydrated to AA over TiO_2 catalyst at 230 °C with a yield of above 95%. Although, the stability of the catalyst and active sites that promotes 3-HPA dehydration have not disclosed in these studies.

Significant deactivation of alumina, silica and titania catalysts in function of time was observed by Kamei *et al.*[123] Fang *et al.* evaluated a variety of solid acid catalysts (HY, ZSM-5, Beta, MCM-41 and silica gel) for dehydration of 3-HPA to produce AA.[124] Among them, commercial silica gel was found to be the most effective to achieve the highest AA selectivity of >99% at complete 3-HPA conversion. The catalyst exhibited excellent stability up to 200 h without deactivation. It was proposed that weak and small amount of Lewis acid sites promote the dehydration of 3-HPA whereas the presence of Brønsted acid sites favors the formation of coke and side products like acetic acid.

Besides the active catalysts, the utilization of highly pure 3-HPA is also essential to achieve better AA selectivity.[125-126, 142] For instance, synthetic derived 3-HPA produced more AA (selectivity 89%) compared to partially purified bio-produced 3-HPA (68%) in bentonite catalysed dehydration reaction.[125] It was found that the impurities present in non-purified bio-3-HPA produce undesired side products that led to fast clogging of the reactor system and reduce overall AA selectivity. In another approach 3-HPA purified by ion-exchange resin prior to dehydration. This process attached traces of phosphoric and sulfuric acid on feedstock surface that can be converted to AA with 98% selectivity at 95% 3-HPA conversion over glass beads in a gas phase reaction.

Thermolysis of poly(3-Hydroxypropionate) over tertiary amine catalysts is another route used to synthesise AA (Scheme 3). This process comprises two steps namely; polymerization of β-propiolactone to poly(3-Hydroxypropionate) in presence of polymerization catalyst (not specified) and thermolysis of the reaction mixture at 150-175 °C by using tertiary amine catalysts to produce AA with 95% yield. Due to the lack of supporting data provided in this patent, no further advancements are available in the literature.

(Scheme 3 here)

Miscellaneous pathways to AA. Other promising pathways to AA utilize allyl alcohol and acetic acid. Allyl alcohol is produced as an intermediate in the transformation of glycerol to AA. Two different catalysts namely molybdenum vanadium mixed oxide and noble metal nanoparticles supported on oxides were reported for the production of AA from allyl alcohol (Scheme 4).

(Scheme 4 here)

As mentioned in the previous section, the surface of molybdenum-vanadium (Mo-V) mixed oxide catalysts comprised heptagonal channels that promote oxidation of acrolein to AA. The reactivity of Mo-V mixed oxide depends upon their crystal structure. For instance, orthorhombic, trigonal and amorphous Mo_3VO_x catalysts produced more AA (>72%) than tetragonal Mo_3VO_x catalysts.[127] This is due to the fact that orthorhombic, trigonal and amorphous Mo_3VO_x catalysts are categorized into analogous structure-type groups. The heptagonal channels present in these rod-shaped catalysts act as an active site for allyl alcohol oxidation. In contrast, tetragonal Mo_3VO_x catalyst does not have heptagonal channels.

Despite the better catalytic activity and selectivity, Mo-V mixed oxide catalysts are not stable. Their activities rapidly decreases with reaction time.[110] The stability of this catalytic system can be increased by the introduction of third metal such as tungsten, copper and iron. Zhang *et al.* doped tungsten within the framework of Mo-V mixed oxide catalyst and

achieved 80% overall yield of AA in the gas phase.[41] They further enhanced the activity of $Mo_8V_2WO_\delta$ mixed oxide catalyst by impregnated on mesoporous silica-supported that produced 90% AA at 340 °C. Both the catalysts were stable even after the reaction time of 100 h. The enhanced activity was explained by the strong interaction between silica and metal oxides that stabilized the active component of $Mo_8V_2WO_\delta$ and improved selectivity.

Recently, Ueda *et al.* doped three metals *i.e.* iron, copper and tungsten separately within the structure of trigonal Mo-V mixed oxide and investigated their activity for allyl alcohol oxidation to AA.[113] Among the tested catalysts, MoVFeO was more active and selective yielded 83% AA at 340 °C. It was found that the local crystal structure around heptagonal channels is important to achieve better AA yield.

Liquid-phase oxidation of allyl alcohol to AA was conducted over noble metal nanoparticles supported on oxide catalysts.[128-129] It was found that the activity of noble metals depends upon kind of support.[128] For example, Au nanoparticles supported on CeO_2 by deposition–precipitation method exhibited better AA selectivity compared to TiO_2, ZnO, Fe_2O_3 and carbon supports. The best result was achieved in a NaOH basic aqueous solution using Au/CeO_2 catalyst with 51% AA yield at 50 °C under molecular oxygen. It was shown that the selective oxidation of allyl alcohol affected by Au oxidation state.

Later, the interaction between Au and CeO_2 supports was improved by using different shaped (rods, octahedral, and cubes) CeO_2 to achieve better AA yield.[130] It was found that the Au nanoparticles deposited on octahedral CeO_2 support (Au/CeO_2-O) showed the highest 92% AA yield in 3M NaOH solution. The excellent activity and selectivity of Au/CeO_2-O catalyst associated with its high surface area and strong metal support interaction.

The oxidation of allyl alcohol typically performed in the presence of a mineral base such as NaOH. However, base-free conditions are needed to decrease the quantity of waste base disposal and facility corrosion. Lee *et al.* proposed an efficient approach to produce AA under base free conditions.[129] In this work different catalysts were prepared by the deposition of noble metal nanoparticles (Au, Rh, Ru, Pt, Pd and Ir) on carbon. Among screened noble metals, Pd nanoparticles deposited on carbon (Pd NP/C) exhibited good activity. Authors have attempted to improve the yield by using different supports and reaction conditions. Under the optimized reaction conditions, maximum 43% AA yield was obtained over Pd NP/C catalyst at 100 °C under molecular oxygen.

Acetic acid is another promising feedstock used to synthesize AA via aldol condensation with formaldehyde (Scheme 5). Acetic acid and formaldehyde are sustainable feedstocks derived by the fermentation of biomass.[131-132] Zeolites, aluminosilicates, supported

alkali and bulk vanadium phosphorus oxides have been proposed for this reaction. For instance, Vitcha *et al.* conducted the condensation of acetic acid with formaldehyde over alkali and alkaline earth metal aluminosilicate catalysts.[133] They obtained 99% AA yield with a high substrate ratio at the reaction temperatures of 275-385 °C. However, the reason for such an excellent activity was not disclosed. Heteroatoms, *e. g.* B, Ti or Sn supported on zeolites such as β, ZSM-5 or MCM-22, have also been tested for this reaction with 90% AA yield.[134]

(Scheme 5 here)

Vanadium phosphorus oxides (VPO) have been extensively used as a catalyst or catalyst support for the production of AA.[135-136] Yang *et al.* found that the relative P/V content is curial because it controls both surface acidity and basicity of the catalyst that influence AA selectivity.[137] When trioxane was used as the formaldehyde source, 98% yield of AA was obtained using the V-P-O catalyst having P/V atomic ratios of 1.06-1.2.[138] However, in case of formalin, AA yield reduced to 75%. Feng *et al.* showed that the fabrication of poly(ethylene glycol) (PEG) additive during the synthesis significantly improved the activity of VPO catalyst .[139] Under the optimized reaction conditions, the highest formation rate (19.8 μmol g_{cat}^{-1} min^{-1}) of AA was accomplished. The achieved AA yield is three times higher than the parent VPO catalyst. It was found that the addition of PEG additive improves the surface area and amount of δ-$VOPO_4$ species that facilitate this reaction.

Doping with other mixed oxides and zeolites is another way to improve the activity of VPO catalysts. Hu *et al.* prepared SiO_2, SBA-15, and HZSM-5 supported vanadium V-P-O catalysts by incipient wetness impregnation method and tested for aldol condensation of acetic acid with formaldehyde to AA.[135] Authors observed that the selectivity of AA significantly affected by support type and P/V atomic ratio. Among the support, SBA-15 showed better selectivity's between 70%-91% at the formaldehyde conversion of 14%-68% with the P/V mole ratio of 2. High surface area and balanced acid base sites were responsible for the improved activity of the V-P-O/ SBA-15 catalyst.

It is possible to synthesize V-P-O catalysts consisting of different phases by tuning the processing temperature. For instance, when ammonium metavanadate and ammonium phosphate precursors calcined at or above 550 °C, pure $VOPO_4$ phase was formed that is less reactive compared to the $(VO)_2P_2O_7$ and $VOPO_4$ phases obtained at slightly lower calcination temperature (500 °C) due to the coexistence of active V^{4+} and V^{5+} species.[140] Yang *et al.* prepared V-P-O catalysts at different temperatures and supported on SiO_2.[141] The V2%−P/SiO_2 catalyst prepared at 500 °C exhibited better selectivity (98%) compared to those

prepared at higher temperatures. However, V2%−P/SiO_2 catalyst produced AA yield of 22% that is not industrially relevant.

To further improve AA yield, Wang *et al.* prepared metallic cation-modified VPO/SiO_2 catalysts by a deposition method. It was found that the ratio of V^{4+} and V^{5+} species increased when Cs, Ce, and Nd cations introduced in the VPO/SiO_2 catalysts. Maximum 74% AA yield by Ce-VPO/SiO_2 catalyst with the formation rate of 10.1 mmol g_{cat}^{-1} h^{-1} at 380 °C was achieved. The excellent activity of the Ce-VPO/SiO_2 catalyst was explained by its moderate acidity and increased V^{4+}/V^{5+} ratios.

Liu *et al.* supported VPO catalyst on three-dimensional siliceous mesostructured cellular foams (MCF).[136] This catalyst was synthesized by depositing VPO precursor $NH_4(VO_2)HPO_4$ on the surface of MCF. During the catalyst synthesis, NH_3 released that was captured on the MCF support surface and automatically induces partial reduction of V^{5+}. It was shown that the surface acidity and V^{4+}/V^{5+} ratios of the supported catalyst can be controlled by tuning the amount of $NH_4(VO_2)HPO_4$ precursor. Through simply tuning the VPO loading on MCF, 84% AA yield was achieved at 360°C.

- **Methacrylic acid (MAA)**

MAA and methyl methacrylate (MMA) are key monomers for poly (methyl methacrylate) (PMMA), which is used to manufacture various end-user products such as electronics, paints and coatings to improve polyvinyl chloride stiffness and artificial bone replacement parts. In 2018, the total available PMMA Market is estimated at ~ $7 billion and anticipated market size of $11.65 billion in 2022, representing a 17% growth.[143] Currently, the majority of MMA is produced *via* the acetone-cyanohydrin (ACH) process.[144] This method uses petroleum-derived feedstocks and concentrated acids. Low atom economy, poor product selectivity and the net emission of greenhouse gases are some drawbacks in the current process.[145]

To overcome these challenges, Mitsubishi Gas Chemicals invented an improved ACH process[146] in which the use of mineral acids and hydrogen cyanide were eliminated. They developed an alternate two-step process to produce MMA and its ester *via* the oxidation of isobutylene and esterification.[147] The alternative methods for the production of MAA include methacrolein esterification, methyl isobutyrate dehydrogenation and aldol condensation of ethyl propionate with formaldehyde.[148-149] Various technologies have been developed to produce bio-based MAA and MMA, though these are at the R&D stage. For instance, Evonik has invested to develop technology for bio-based MAA. In the following sections, we discuss

different catalytic approaches that have been utilized for the production of MAA from biomass derived sources.

MAA production from different bio-based feedstocks

Isobutane to MAA. The bio-based production of isobutane through thermo-catalytic method is known since 1970s.[150] The catalytic method to produce MAA via oxidation of isobutane has gained a lot of attention in recent years. In this process methacrolein is formed as an intermediate (Scheme 6). This section summarizes the latest developments to produce MAA selectivity.

(Scheme 6 here)

(Table 2 here)

Keggin-type $H_4PVMo_{11}O_{40}$-based catalysts are most active and selective for the gas-phase oxidation of isobutane to MAA due to their flexible structure in which the acidity or basicity of the catalysts can be easily tuned by incorporating appropriate transition metals. In the general Keggin type structure, the phosphorus atom located at the centre in tetrahedral environment is surrounded by 12 octahedra units of MoO_6. The oxygen atoms are shared corners by molybdenum atoms through covalent bond, except for 12 terminal oxygen atoms (O_t) attached to only one addendum atom (Mo). Bulk $H_4PVMo_{11}O_{40}$ catalyst demonstrated poor performance in isobutane conversion due to its low surface area and acidity (Table 2, entry 1).[145] In contrast to the bulk $H_4PVMo_{11}O_{40}$ catalyst, its reduced form showed better MAA selectivity.[151] Ueda *et al.* formed a highly reduced heteropoly molybdophosphate catalyst ($H_3PMo_{12}O_{40}$-Py) by the heat-treatment of pyridinium or quinolinium salts that produced MAA with 58% selectivity at 12% conversion of isobutane (Table 2, entry 2).[152] An improved MAA selectivity was explained by a highly stable reduced state and structure of the $H_3PMo_{12}O_{40}$-Py catalyst.

Incorporation of metal ions such as cesium (Cs^+), ammonia (NH_4^+), vanadium (V^{5+}), copper (Cu^{2+}) and iron (Fe^{3+}) into the parent $H_3PMo_{12}O_{40}$ catalyst is another effective way to improve MAA selectivity.[153] Partial substitution of H^+ ion with Cs^+ in $H_3PMo_{12}O_{40}$ showed improved catalytic performance.[154] For instance, Mizuno *et al.* conducted oxidation of isobutane over $Cs_xH_{3x}PMo_{12}O_{40}$ catalysts under isobutane lean and rich conditions. They achieved optimum 24% MAA selectivity at 16% isobutane conversion under isobutane-lean conditions, whereas, isobutane-rich conditions result in low MAA selectivity (6.5%) and isobutane conversion (3.9%), respectively(Table 2,

entry 3). Other compositions for Cs^+ substituted $H_3PMo_{12}O_{40}$ catalysts have also been proposed, but they demonstrated poor catalytic performance (Table 2, entries 4-5).[155-156]

Ammonia substituted $H_4PVMo_{11}O_{40}$ catalysts have been investigated for isobutane oxidation under both isobutane rich and isobutane-poor conditions. Cavani *et al.* found that under isobutane-rich conditions, higher selectivity to MAA (43%) was obtained over the $(NH_4)_3PMo_{12}O_{40}$ catalyst (Table 2, entry 6).[157] Under isobutane-poor conditions, the selectivity of MAA was much lower (4%) with the same catalyst. In case of isobutane-rich conditions, redox reaction between ammonia and Mo^{6+} occurred that significantly improved the catalyst performance. The main disadvantage of this catalytic system is that more than 80 h was required to reach a steady state. pH of the synthetic solution during the catalyst preparation is also the key parameter that affects activity of the catalyst.

The inclusion of vanadium into the structure of heteropoly molybdophosphate has significantly improved MAA selectivity.[145] The partial substitution of molybdenum with vanadium improved the redox properties of $H_3PMo_{12}O_{40}$ heteropoly acids. In the structure of the $H_4PVMo_{11}O_{40}$ catalyst, vanadium occupies the cationic position and acts as an active site for isobutane oxidation.[158] By using this catalyst, up to 30% MAA selectivity at 11% isobutane conversion can attend(Table 2, entry 7).[159a] The effect of Cs^+ and NH_4^+ ions doping on the activity of the $H_4PVMo_{11}O_{40}$ catalyst was also investigated by several researchers. Liu-Cai *et al.* observed a volcano-type behavior with respect to a cesium content and MAA selectivity over the $Cs_xH_{1-x}VO$-$(PMo_{12}O_{40})$ catalysts.[159b] The authors achieved maximum 76% selectivity of MAA and methacrolein (MAC) at cesium amount of x = 0.75 with $Cs_{0.75}H_{0.25}VO(PMo_{12}O_{40})$ catalysts. They explained that the Brønsted acid sites on the surface of the catalyst played a crucial role in the reaction.

In addition to the amount of cesium, the precursors used to prepare the catalyst are also important. Recently, Yang *et al.* prepared a series of vanadium-substituted cesium salt of heteropoly compounds by using three different precursors *i.e.* vanadyl oxalate, vanadyl sulphate and vanadium acetylacetonate (Table 2, entry 8).[160] They found that the catalysts prepared from vanadyl sulphate have suitable surface V^{4+}/V^{5+} ratio and higher surface acidity compared to the other precursors that results in 55% MAA selectivity.

Simultaneous insertions of cesium and ammonia within the structure of the $H_4PVMo_{11}O_{40}$ catalyst have also been studied.[161-162] Paul *et al.* investigated the effect

of ammonia/cesium ratios on the catalytic activity of $Cs_x(NH_4)_{3-x}HPMo_{11}VO_{40}$ mixed salts.[163] A strong correlation between ammonia/cesium ratios and the specific surface area was observed. The addition of cesium stabilized the Keggin structure and prevented the elimination of V atoms from the primary structure. Under the optimized reaction conditions, a maximum 57% selectivity to MAA and MAC was achieved at 10% isobutane conversion over the $Cs_{1.7}(NH_4)_{1.3}HPMo_{11}VO_{40}$ catalyst (Table 2, entry 9). The result was explained by the balance acidic properties and high specific surface area.

Later, they dispersed different amounts (10-50 wt.%) of $(NH_4)_3HPMo_{11}VO_{40}$ (APMV) active phases on cesium-containing heteropoly salts ($Cs_3PMo_{12}O_{40}$) and evaluated for isobutane oxidation.[162] They found that the selectivity of MAA depends on APMV amount and can reach maximum (47%) with 50 wt.% APMV loading (Table 2, entry 10). A strong correlation between the amount of strong acidic sites and MAA selectivity was observed.

The addition of iron within the structure of $H_3PMo_{12}O_4$ also increased the selectivity of MAA. Millet *et al.* found that H^+ ion substituted $Fe_{0.85}H_{0.45}PMo_{12}O_{40}$ exhibited improved catalytic activity.[155] In this reaction partially iron enhanced the activity of the acid phase produce MAA with 9% selectivity (Table 2, entry 11). Interestingly, when iron introduced in the cesium salts, it only improved MAA selectivity without effecting isobutane conversion.[164] Iron increased the transformation of isobutane from MAC to MAA and suppressed the formation of side products. The effect of iron doping on the activity of cesium salts ($Cs_{2.5}FexH_{0.53x}PMo_{12}O_{40}$) under isobutane-rich and poor condition was investigated by several researchers (Table 2, entries 12-13).[154, 165-166] However, the excess iron loading creates strong Lewis acid centers within the catalyst that reduced the selectivity of MAA.[167]

Copper is another metal that exhibits a positive effect on MAA selectivity. Langpape *et al.* found that the addition of copper in phosphomolybdic heteropoly acid compounds positively improves the activity of the catalyst.[168] Mizuno *et al.* also shown that the addition of copper in $Cs_{2.5}H_{0.5}PMo_{12}O_{40}$ heteropoly acid improve the activity and selectivity by promoting the re-oxidation of the catalyst under isobutane-rich conditions (Table 2, entry 14).[169] Yang *et al.* recently co-substituted VO^{2+} and different transition metals (Cu, Fe, Ni and Ce) in Cs-Salts of the Keggin-type phosphomolybdic acid.[170] Among them, $Cs_{2.0}V_{0.3}Cu_{0.2}PMo_{12}O_{40}$ catalyst prepared by co-incorporation of VO^{2+} and copper exhibited higher catalytic performance. A maximum, 47% MAA

selectivity at 13% isobutane conversion was obtained. This was explained by catalyst re-oxidation due to the synergistic effect of Cu^{2+} and VO^{2+} (Table 2, entries 15-16). Wang *et al.* explained that the electron transfer mechanism between copper and molybdenum contributed to the positive effect of the copper loading.[171]

Besides Keggin-type heteropoly acids, few mixed oxides have also been proposed for the oxidation of isobutane. For instance, Kan *et al.* prepared a series of $MoV_{0.3}Te_{0.25}Sb_x$ (x = 0–0.6) mixed oxide catalysts by a hydrothermal synthesis route. The maximum isobutane conversion of 15% at 12% MAA selectivity was obtained over the $MoV_{0.3}Te_{0.25}$ catalyst, whereas $MoV_{0.3}Te_{0.23}Sb_{0.5}$ catalyst promoted the oxidation of isobutane to MAC with 48% selectivity(Table 2, entry 17).[172] Guan *et al.* studied the effect of cesium and molybdenum on the catalytic activity of V-Ce-Te mixed oxides.[173] It showed molybdenum activated isobutane, whereas Ce ions likely modified the redox process of the catalysts and performed selective oxidation of isobutane. Under optimal reaction conditions, $MoV_{0.3}Te_{0.23}Ce_{0.2}$ achieved the best methacrolein and MAA selectivity (53%) and yield (10%) at 420 °C (Table 2, entry 18).

Bio-based carboxylic acids to MAA. Biomass-derived carboxylic acids are promising monomers for plastics, paints and coating applications.[174] Bio-based MAA is produced by dehydration and decarboxylation of bio-based carboxylic acids such as IA, citric acid, and aconitic acid. Citric acid and IA are derived from the fermentation of carbohydrates. Many significant improvements have been made for the highly selective transformation of sustainable carboxylic acids into MAA by using both homogeneous and heterogeneous catalytic systems. We have reviewed both catalytic systems in the following sections.

Homogeneous Catalysts. In the homogeneous catalytic system, active sites of the catalyst can interact efficiently with the reaction substrate because both are in the same phase. This interaction resulting in high product yield compared to heterogeneous catalysts. The first report on catalytic dehydration and decarboxylation of citric acid and itaconic acid (IA) to MAA over homogeneous catalysts was published in 1994 by Magnus Carlsson and his group .[175] Authors have performed initial sets of experiments under near-critical and supercritical water conditions. When citric acid is exposed to hot (320 °C) compressed (34.5 MPa) water, it is converted to 7% MAA and 35% IA and several side products such as citraconic acid, acetone and acetic acid were formed under similar substrate concentration (Table 3, entry 1). IA yields 30% MAA at 400 °C with the main byproducts being citraconic acid, mesaconic acid and acetic acid (Table 3, entry 2). Under the reported reaction conditions dissociation of water into hydronium and hydroxide ions promotes decarboxylation of acids.

It was observed that the reaction temperature and pH of the reaction mixture are two important factors that affect the yield of MAA. Under neutral conditions, high temperature (>250 °C) promotes parasitic reactions, which leads to produced acetone and acetic acid byproducts. Lower pH favored the parasitic reactions from IA, whereas higher pH quenched the decarboxylation reaction. The optimum yield of MAA (70%) was achieved from 0.05-0.1 M IA in 10 s at 360 °C in the presence of 0.2M NaOH (Table 3, entry 3).

In 2015, Lucite International filed patent inventions in which different bio-based carboxylic acids have utilized to produce MAA. Maximum 52% MAA yield was claimed when mesaconic acid was used as a substrate, whereas 40% and 49% MAA yields were obtained for citraconic acid and IA, respectively, over 0.5M NaOH at 300 °C (Table 3, entry 4).[176] When mesaconic acid and citraconic acid were used as substrates, the respective MAA yields were 52% and 42% MAA (Table 3, entries 5-6).

The Brill group reported that the rate of the decarboxylation of IA is pH dependent.[177] Low pH favors the hydrolytic degradation of IA that results in the formation of side products such as acetic acid, acetone and reduces the yield of MAA (Table 3, entry 7). Alkaline pH also influenced MAA selectivity. The hydroxide ions at high pH participate in the parasitic reaction pathway by the hydrolysis of IA. It was found that the yield of MAA significantly enhanced when citraconic acid was employed as a sustainable feedstock (Table 3, entries 8-9). In the homogenous catalyzed decarboxylation approaches, NaOH promotes the reaction by abstracting the proton from carboxylic acid.[175-176]

Despite the promising results, utilization of such corrosive alkaline base is not viable on an industrial scale due to the toxicity, purification and separation issues. In addition, high reaction temperature (>250 °C) is required to achieve better MAA selectivity. In order to overcome such limitations ruthenium carbonyl propionate and Mn(II) oxalate were used as homogenous catalysts for the decarboxylation of IA.[178] High selectivity (>90%) to MAA was achieved over ruthenium carbonyl propionate at 0.1 mol.% catalyst loading and high IA concentration (5.5 M) at low temperature and pressure (Table 3, entry 10). The Mn(II) oxalate catalyst yielded 5% MAA due to the decomposition of oxalate to carbon monoxide gas. An attempt has also been made to improve the yield of MAA by the addition of triphenylphosphine as a catalyst stabilizer, which exhibited a greater catalytic efficacy (14% yield). In all the experiments authors have used tetraglyme as a co-solvent that significantly lowered the vapour pressure of water and prevent the decomposition of starting acids. However, the reasons for such an impressive result at low temperatures have not mentioned.

(Table 3 here)

Heterogeneous Catalysts. Homogeneous catalysts have disadvantages including expensive recovery to recycle and reuse. The Scott group from the Wageningen University & Research Centre, Netherlands made significant advancements on the utilization of heterogeneous catalysts for the decarboxylation of biomass derived carboxylic acids to MAA.[179] Several solid transition-metal catalysts have been developed and tested under the reaction conditions that are relatively milder compared to those reported previously (Table 4).[178] In this reaction NaOH was used as a co-catalyst that reduced the formation of unwanted side products. Pd based catalyst achieved slightly lower selectivity to MAA due to subsequent decarboxylation steps that forms side products (Table 4, entries 1-3). Under similar reaction conditions, a Ru based catalyst performed poorly and promotes parasitic reactions. The best MAA selectivity (84%) was obtained with a Pt/Al_2O_3 catalyst at 250 °C (Table 4, entry 4). Hence, the scope of the Pt/Al_2O_3 catalyst was extended for the conversion of citric acid and aconitic acid, which produced 41% and 47% of MAA, respectively (Table 4, entries 5-6). Pt/Al_2O_3 has a positive stabilization effect on the itaconate monoanion that allow selective production of MAA.

In order to avoid the use of hazardous alkali solution and costly noble metals, the Pirmoradi's group tested hydrotalcite as a heterogeneous catalyst to obtain MAA from IA citric acid and 2-hydroxyisobutyric acid (2-HIBA) in subcritical water.[180] 2-HIBA, produced by fermentation of renewable feedstock, is an interesting building block for polymer.[181] Significantly higher MAA yield (71%) was achieved from 2-HIBA dehydration in short residence time (1 min) and at 275 °C (Table 4, entry 7).

.The yield of MAA decreased at higher residence time due to the degradation of MAA in the acidic subcritical reaction medium. However, the yields of MAA from citric acid (21%) and IA (23%) were lower (Table 4, entries 8-9). Authors reveal that the presence of the medium and strong basic sites on the surface of the catalyst promotes 2-HIBA dehydration. In case of citric acid and IA, Lewis acid sites contribute to the dehydration of citric acid to IA followed by decarboxylation to MAA.

Inspired by this work our research group recently reported noble metal free heterogeneous catalysts for the conversion of biomass derived carboxylic acids (citric acid, IA and aconitic acid) into MAA.[182] In this report we have synthesized high surface area hexaaluminate catalysts by adopting carbon templating route and tested for the decarboxylation reaction. The utilization of carbon as a hard templating agent inhibits the agglomeration of the particles during calcination and yields catalyst with the high surface area.[183]

In the initial screening experiments we have found that calcium hexaaluminate (CHA), lanthanum hexaaluminate (LHA), and magnesium hexaaluminate (MHA) are comparatively less active than barium hexaaluminate (BHA) catalyst (Table 4, entries 10-12). This is due to the high basicity and low surface area of the catalysts. It was found that high temperature (>250 °C) and pressure (>20 bar) have a negative effect on MAA selectivity under our catalytic system. High temperature prevents adsorption of substrate on the catalyst surface, whereas high pressure decomposes MAA into side products.

We have achieved 50% yield of MAA over barium hexaaluminate catalyst (BHA) at 250 °C temperature under the 20 bar pressure of nitrogen (Table 4, entry 13). We have also explored the scope of BHA catalyst for the production of MAA from citric acid and aconitic acid. Under the optimized reaction conditions, 50% and 51% yields of MAA were obtained from citric acid and aconitic acid, respectively (Table 4, entries 14-15).

The structural investigation suggested that the high activity of BHA catalyst is associated with its peculiar layered structure, presence of ordered surface defect sites, high specific surface area and moderate basicity.

In order to show the industrial applicability of the as-prepared bio-based MAA, we have performed copolymerization of MAA to prepare acrylic emulsions that are widely used in coating industry.[184] We have also compared the physical and chemicals properties of bio-MAA based copolymer with petroleum derived MAA based copolymer and found no difference in their properties.

(Table 4 here)

- **Styrene (ST)**

ST is an industrially important commodity chemical, which is widely used to produce polystyrene plastic, polyesters, protective coatings, resins, rubbers and other copolymers.[185] The chemical structure of ST contains an active vinyl group that can be further functionalized for the synthesis of versatile synthetic intermediates. In 2017, the global production of ST was 15 million tons with a total market size of approximately $43.1 billion.[186] ST was first isolated in 1839 by Eduard Simon, an apothecary in Berlin, from distilled storax resin obtained from the ‘Tree of Turkey’ and named styrol.[187] The industrial production of ST from dehydrogenation of ethylbenzene was started from 1940. This section summarizes different catalytic approaches to produce ST.

ST production from bio-based feedstock

Bio-based ethylbenzene to ST. Bio-based ethylbenzene can be produced from lignin and lignocellulosic biomass.[188] The current bio-refinery processes create value added products from carbohydrates, leaving lignin as a waste.[189] The estimated lignin generation as a by-product from the paper and pulping industries is about 70 million tons per year,[190] which is mostly burned for heat and imparts serious environmental concerns. However, lignin contains natural aromatic/phenolic compounds.[190] Li *et al.* reported a process to produce bio-based ethylbenzene through depolymerization of lignin into aromatic monomers followed by selective alkylation of the monomers to ethylbenzene (72% yield). [191] Several research articles have been published on sustainable production of ethylbenzene from lignocellulosic biomass. [192]Although ethylbenzene is not currently produced on commercial scale, this article provides an outlook on how a matured bio-based ethylbenzene production technology can be integrated into the current ST production process.

The oxidative dehydrogenation of ethylbenzene to ST can be performed at low temperature and the reaction is not an equilibrium-limited. Several mild oxidizing agents such as O_2, CO_2, N_2O and SO_2 have been used for low-temperature oxidative dehydrogenation of ethylbenzene.[193] CO_2 is a soft oxidant, which was adopted for the first time by Sugino in 1995. [194] The reaction was carried out over an activated carbon supported iron catalyst, which yielded 45% ST with 90% selectivity at 550 °C in 5 h of reaction time. Apart from a notable positive impact on carbon emissions, the utilization of CO_2 can offer several advantages such as the acceleration of reaction rate, acting as a diluent, enhancing product selectivity and thermodynamic stability.[195] The oxidative dehydrogenation of ethylbenzene in CO_2 was preceded through the two-step reaction pathway. H_2 from the dehydrogenation step simultaneously undergoes reverse water-gas shift (RWGS) reaction with CO_2.[196]

Vanadium based catalysts have been used extensively for homogeneous and heterogeneous catalytic oxidative dehydrogenation of ethylbenzene.[197-198] The oxidative dehydrogenation of ethylbenzene in the absence of CO_2 leads to the formation of undesired side products and facilitates faster deactivation of the catalyst.[199] It was found that CO_2 promotes the stability of the catalyst and improves selectivity to ST. Additionally, CO_2 acts as a soft oxidant as well as diluent and lower the partial pressure of reactants.[200]

A plausible mechanism for oxidative dehydrogenation of ethylbenzene over the vanadium catalysts in the presence of CO_2 involved an interaction between V-O bond of the catalyst and alkyl hydrogen atoms of ethylbenzene, wherein abstraction of hydrogen from ethylbenzene took place. Afterward, a nucleophilic attack of ethylbenzene with the V^{5+} sites

forms ST (Scheme 7).[201] The vanadia catalysts supported on Al_2O_3, SiO_2, ZrO_2, WO_3, MgO, SBA-15 and carbon have been reported for oxidative dehydrogenation of ethylbenzene to ST at reaction temperatures ranging from 530 to 600 °C under atmospheric pressure.[29, 202] It was found that the catalytic performance depends upon the catalyst's supports, support surface areas, and loading amount of vanadium active metals.[203]

(Scheme 7 here)

Among various supports alumina has a major contribution to oxidative dehydrogenation of ethylbenzene because of its chemical and thermal stability, better redox properties, strong support-catalyst interaction and high specific surface area. Table 5 summarizes the literature data for ST production over vanadium based catalysts. Using a V/γ-Al_2O_3 catalyst, Makkee *et al.* reported a ST selectivity of 92% after 15 h of reaction at 600 °C in a fix bed reactor using 10 vol.% ethylbenzene as a feed (Table 5, entry 1).[204] The deactivation of the catalyst was observed due to the coke formation on the support surface. Similar deactivation was observed when other transition metals (Cr, Sn, Ni, Zr, Sn and Mn) doped in γ-Al_2O_3 support. [205]

(Table 5 here)

Li *et al.* used ordered mesoporous alumina-supported vanadium oxides and 97% selectivity to ST was obtained at 550 °C for 12 h (Table 5, entry 2).[203] Unlike the V/γ-Al_2O_3 catalyst, the ordered mesoporous alumina (OMA) supported vanadia catalyst (V/OMA) exhibited superior catalytic performance and prevented the coke formation. OMA facilitated stabilization of highly dispersed V^{5+} active species in the catalyst. The deactivation of the catalyst can also be prevented by coating a thin carbon layer on the Al_2O_3 surface.[206] The possibility of using TiO_2 along with Al_2O_3 as a support was explored by Nagaraja *et al.* in 2017.[207] By using a V_2O_5/TiO_2-Al_2O_3 catalyst, maximum conversion of ethylbenzene and ST selectivity were 65% and 96%, respectively, at 550 °C and a notable stability of the catalyst was observed up to 60 h with CO_2 (Table 5, entry 3). Hexagonal mesoporous silica (HMS) is another promising support for the synthesis of vanadium based catalyst. A report by Rabie *et al.* using VO_x-modified hexagonal mesoporous silica (VO_x/HMS) catalyst demonstrated the feasibility of performing the oxidative dehydrogenation of ethylbenzene.[202] It was observed that the selectivity of ST depends upon the concentration of vanadium and reached maximum (99%, ST) at 20 wt.% vanadium content (Table 5, entry 4).

Various promoters, such as Li, K, Mg, Ce, Co, La, Cr and Zr have been incorporated on V/Al_2O_3. Park *et al.* reviewed the role of various promoters incorporated in solid oxide

catalysts for ST production (Table 5, entries 5-9).[208] Among the promoters investigated, Cr and Mg incorporated catalysts showed an evidently positive effect on the ST selectivity because of the better redox properties.

The application of mixed metal oxides for oxidative dehydrogenation of ethylbenzene has received considerable attention in recent years.[209] Table 6 summarizes the activity of the mixed oxide catalysts for the conversion of ethylbenzene to ST, where the reaction temperature ranges between 475 °C and 660 °C and CO_2 was used as an oxidant under atmospheric pressure. Pure oxides of manganese (MnO_2) and zirconia (ZrO_2) and MnO_2-ZrO_2 mixed oxides have been used for the reaction.[210] The binary MnO_2-ZrO_2 oxide catalyst exhibited excellent catalytic activity compared to those of individual oxides. Maximum 98% selectivity to ST at 73% ethylbenzene conversion over 10% MnO_2-ZrO_2 mixed oxide catalyst was achieved at 600 °C, which was attributed to their high surface area (Table 6, entry 1).

(Table 6 here)

Park *et al.* disclosed ethylbenzene oxidative dehydrogenation using different compositions of TiO_2-ZrO_2 binary metal oxides and the modified binary oxides incorporated with potassium oxide (K_2O).[211] In the latter case, K_2O acted as a basic promoter and improved the conversion of ethylbenzene and selectivity to ST. Using K_2O/TiO_2-ZrO_2, ST selectivity of up to 99% with 65% ethylbenzene conversion was obtained at 660 °C (Table 6, entry 2). In another study, Park *et al.* showed that a Na incorporated catalyst exhibited the best selectivity to ST due to the enhancing the surface basicity of the catalyst and also the labile oxygen species.[196] Using a Na-24/TiO_2-ZrO_2 catalyst, 72% conversion and 97% selectivity to ST were obtained (Table 6, entry 3). The highest activity of the Na-24/TiO_2-ZrO_2 catalyst compared to K-24/TiO_2-ZrO_2 and TiO_2-ZrO_2 catalysts can be attributed to the higher basic sites and formation of $TiZrO_4$ solid solution, which has higher concentration of active sites for the activation of both CO_2 and ethylbenzene. Nagaraja *et al.* reported the high efficiency of a MoO_3/TiO_2-Al_2O_3 catalyst for selective oxidative dehydrogenation of ethylbenzene to ST.[261] In 1 h and at 650 °C, ST was obtained with a selectivity of 96% at 77% conversion of ethylbenzene (Table 6, entry 4). V_2O_5, and CeO_2 doped TiO_2-ZrO_2 mixed oxide catalysts were also used in the reaction.[212-214] It was found that the addition of CeO_2 to V_2O_5/TiO_2-ZrO_2 prevented the deactivation of the catalyst, enabling high catalyst stability, and better catalytic activity. Among all tested catalysts, 99% selectivity to ST at 60% ethylbenzene conversion was achieved over the V_2O_5-CeO_2/TiO_2-ZrO_2 catalyst at 600 °C. Recently Rao *et al.* developed a Co_3O_4 doped $MgAl_2O_4$ catalyst for ethylbenzene dehydrogenation.[215]

Ethylbenzene conversion of 81% with 98% selectivity to ST was attained over the $1.0Co_3O_4/MgAl_2O_4$ catalyst (Table 6, entry 5).

Ceria is one of the extensively used catalysts for oxidation reactions due to its high oxygen storage capacity, which is derived from the redox cycle between Ce^{4+} and Ce^{3+}.[216] In 2015, Li *et al.* used $Ce_xZr_{1-x}O_2$ mixed oxide catalyzed oxidative dehydrogenation of ethylbenzene.[217] It was found that $Ce_xZr_{1-x}O_2$ catalysts attained higher ethylbenzene conversion than pure CeO_2. The best reaction conditions achieved a maximum conversion of 55% and ST selectivity of >86% in the presence of CO_2 at 550 °C over a $Ce_{0.5}Zr_{0.5}O_2$ catalyst (Table 6, entry 6). Recently, Liu *et al.* revealed that the defects and the redox cycle between Ce^{3+}- Ce^{4+} were two important factors for high performance of $Ce_{1-x}Zr_xO_2$. Park *et al.* investigated the influence of ceria on structural and catalytic properties of TiO_2-ZrO_2 mixed oxide.[218] The catalysts promoted with ceria exhibited more Brønsted acid sites. Among the catalysts tested, the microwave treated CeO_2/TiO_2-ZrO_2 sample exhibited the highest ethylbenzene conversion (74%) and a remarkable ST selectivity (98%) at 600 °C (Table 6, entry 7).

Nagaraja *et al.* used SBA-15 supported CeO_2-ZrO_2 catalyst for the dehydrogenation of ethylbenzene to ST with CO_2.[219] A screening of the catalysts (CeO_2, ZrO_2, cerium–zirconium mixed oxide, SBA-15 and 25/25CZS) revealed that a 25/25CZS (containing CeO_2, ZrO_2 and SBA-15) catalyst with 75 wt.% SBA-15 doping gives a good conversion of ethylbenzene and selectivity to ST, which is attributed to the high surface area and surface basicity of the catalyst. After 10 h of reaction at 650 °C under CO_2, up to 93% selectivity to ST was obtained (Table 6, entry 8). Feng *et al.* reported ceria doped with Fe catalyst ($Ce_{0.8}Fe_{0.2}O_2$), which was found to be an efferent catalyst for selective ethylbenzene conversion (45%) to ST with high selectivity (98%) (Table 6, entry 9).[220] Raja *et al.* employed a cerium containing mixed oxides derived from hydrotalcites to dehydrogenate ethylbenzene.[221] They obtained 97% selectivity to ST over MAC-2 with excellent catalyst stability for at least 12 h (Table 6, entry 10). The excellent catalytic activity was attributed to the basicity, reducibility, oxygen storage capacity and metal surface concentration of the catalyst.

Alumina is also used in many studies as a catalyst or catalyst support for oxidative dehydrogenation of ethylbenzene to ST.[222] The high surface area and moderate basicity of alumina played a crucial role in dehydrogenation of ethylbenzene. A recent report by Petrov *et al*. shows that the catalytic activity of alumina-based catalysts can be improved by the promotion with boron (B) and antimony (Sb).[223] Interestingly, alumina alone gave only 58% selectivity to ST at 32% of ethylbenzene conversion. In the presence of 15 mol.% of B to Al

significantly enhanced the selectivity of ST to 94% at 46% ethylbenzene conversion and at a reasonably low temperature (475 °C) (Table 6, entry 11). The mixed oxides based on aluminate and silicate have also reported for the production of ST (Table 6, entries 12-14).[207, 262-263]

Carbon nanotube (CNT), graphene and nanodiamond (ND) are promising and inexpensive materials compared to the metal oxide catalysts for the production of ST [224-225] Nanocarbons have several advantages over metal oxides. The large pore diameter, high surface area, and tunable acidity or nanotube can minimize coke formation.[226] In 1990, a new class of catalysts based on earth-abundant carbon materials was discovered as an efficient, low-cost, and metal-free alternative for ST production.[227] These carbon-based catalysts were prepared by the pyrolysis of polyacrylonitrile at 400 °C. Among the tested catalysts, carbon molecular sieves (AX-21) in particular, exhibited extraordinary reactivity. Under an optimized reaction conditions and at 350 °C, 90% selectivity to ST was obtained at 80% conversion of ethylbenzene (Table 7, entry 1). In 2001, Serp *et al.* prepared a multi-walled carbon nanotubes (MWNT) by different oxidative treatments and evaluated its catalytic activity in the ethylbenzene oxidative dehydrogenation to ST.[228] It was found that a pre-oxidized MWNT (NT1) is more active for oxidative dehydrogenation in the initial stage of the reaction produced styrene with 59% selectivity (Table 7, entry 2).

(Table 7 here)

Su *et al.* studied the effect of the microstructure of carbon nanotubes (CNTs) on the oxidative dehydrogenation of ethylbenzene to ST.[229] The CNTs were treated at different temperatures to tune the oxygen containing functional groups on the surface. The CNTs treated at 700 °C (CNT700) exhibited 50% ethylbenzene conversion and 65% ST yield at 500 °C (Table 7, entry 3). This activity is attributed to the presence of oxygenated functional groups on the surface of the catalyst. CNTs treated above 1500 °C leads to oxygen-free surface with a low number of structural defects and showed low catalytic performance in comparison to those treated below 1100 °C with a higher number of oxygen functionality. The oxidative treatment of CNTs generated various surface functional groups such as carboxylic (-COOH), carbonyl (-C=O) and hydroxyl groups (-C-OH).[230] This treatment was performed under harsh conditions, e.g. utilization of hot nitric acid or mixture of concentrated acid with strong oxidant ($H_2SO_4/KMnO_4$) that can lead to damage the structure of CNTs.[231]

Ondruschka *et al.* used an advanced oxidation process, which employed the UV light and hydrogen peroxide as an oxidant, to prepare oxygen rich CNTs.[232] The resulting UV/H35 MWCNTs catalyst gave 47% conversion of ethylbenzene and high selectivity to ST (up to

91%) (Table 7, entry 4). Wang *et al.* reported a facile synthesis method of boron carbonitride nanosheets (BCN), containing hybridized, randomly dispersed domains of hexagonal boron nitride and carbon (such as graphene) by the pyrolysis process.[233] As-synthesized carbon-doped boron nitride nanosheets possessed excellent stability and high ST selectivity (89%) at 500 °C after 30 h reaction (Table 7, entry 5).

Nano-structured diamond-based carbon materials have recently received a great attention as a heterogeneous catalyst for different chemical transformation because of its unique sp^3-sp^2 core-shell structure, high surface area and excellent thermal and mechanical stability.[234] In 2010, Su *et al.* described the application of nano-diamond as a novel catalyst for dehydrogenation of ethylbenzene under steam-free conditions.[235] The authors revealed that unique structural defects of sp^2/sp^3-hybridized bucky nano-diamond (BND) structures are likely responsible for the enhanced activation rate in ethylbenzene dehydrogenation.

In 2014, Zhao *et al.* developed a nano-diamond/carbon nitride hybrid catalyst (ND/CNx-750) and achieved 99% ST selectivity at 550°C in a fixed-bed reactor (Table 7, entry 6).[236] In 2016, Pham-Hu *et al.* synthesized hierarchical carbon nanofibers/grapheme composite containing nanodiamonds (ND/CNF-FLG) by chemical vapor deposition and tested for the direct dehydrogenation of ethylbenzene.[237]An excellent ST selectivity of 93% was obtained over a hybrid ND(16%)/CNFFLG catalyst at 575 °C with 39% ethylbenzene conversion (Table 7, entry 7). The catalyst exhibited high stability for 70 h on the time-of-stream study. In the same year, Su *et al.* achieved significant improvement to ethylbenzene conversion by combining the oxidative and non-oxidative dehydrogenation of ethylbenzene in one reactor under oxygen lean conditions over a nano-diamond as a metal free catalyst.[238] The nano-diamond catalyst (ND) demonstrated about 40% ethylbenzene conversion with 92% ST selectivity at 450 °C temperature and maintained stability even after 240 h of time-of-stream study (Table 7, entry 8). In another work, Zhao *et al.* prepared carbon nitride encapsulated nano-diamond hybrid (H-ND) catalyst for ST production from ethylbenzene.[239] The catalyst was prepared through mechanical milling of nano-diamond powder and hexamethylenetetramine followed by pyrolysis of the mixture. The catalyst was stable up to 50 h and produced ST with 99% selectivity (Table 7, entry 9).

Recently, Zhou *et al.* demonstrated a superior performance of defect-enriched nitrogen and oxygen co-doped nano-diamond/carbon nanotube catalyst (N,O-ND/CNTd) in ethylbenzene dehydrogenation.[240] At 550 °C, as-prepared N, O-ND/CNT-d gave 98.7% selectivity to ST at a steady-state ST formation rate of 5.2 mmol g^{-1} h^{-1} (Table 7, entry 10). Su *et al.* developed an efficient novel type of metal-free carbon-based monolith catalysts

(ND@NMC-0.02P/SiC) for ethylbenzene dehydrogenation.[241] Under the optimized reaction conditions, this catalyst demonstrated better catalytic performance produced ST with 90% selectivity at 32.6% ethylbenzene conversion (Table 7, entry 11).

- **Conclusions and future prospects**

Production of drop-in and functional replacement bio-products, as well as bio-based platform feedstocks from lignocellulosic biomass has received significant attention over the past decade. In parallel, research and commercialization focus on the transformation of bio-based feedstock (*e.g.* platform chemicals) into various monomers for bio-based plastics is advancing, although at a slow pace in some cases. Multistep processing of recalcitrant lignocellulosic biomass having complex chemical structure often makes drop-in-replacement bio-products less competitive to petroleum analogues. Therefore, long term research and commercialization investment are necessary to understand complex structures, develop a process-intensification approach to enable drop-in replacement bio-products cost-competitive and produce functional monomers, e.g. vinyl-based compounds, allowing next generation bio-based and bio-degradable plastic industries possible. This article presents a concise review of recent catalytic developments to produce AA, MAA and ST monomers. AA is currently produced from petroleum-derived propylene through energy intensive multiple step processes.

Various multicomponent catalysts and sustainable feedstocks have been proposed for the sustainable production of bio-based AA. Among different feedstocks, glycerol and LA have the potential to replace petroleum-based propylene. The production of AA by single or two-step approaches would be a decent alternative. However, the utilization of commercially available glycerol as a feedstock is not economic. To reduce the production cost, crude glycerol obtained as a by-product of biodiesel from biorefineries was employed. Nevertheless, the impurities present in the crude glycerol deactivated the catalyst. The catalyst deactivation can be efficiently inhibited by using molecular oxygen as an oxidant.

LA is other promising feedstocks derived in high yield from glycerol and more mature fermentation routes. However, controlling this reaction for the selective production of AA is difficult because several reactions such as decarbonylation and decarboxylation occur during the transformation. Several zeolites, phosphates and sulphates have proposed for the gas-phase dehydration of LA to AA. Among them phosphates are more active and resistance to deactivation. However, further research is needed to identify the active sites of the catalyst that promotes LA dehydration.

Isobutane and carboxylic acids are the two major feedstocks for MAA. Keggin-type heteropoly compounds (HPC) are widely used for the oxidation of isobutane because of their acidity and redox characteristics. Metal ions can tune the acidity of the HPC catalysts to control the catalytic performance, which depends upon the type of metal ions inserted within the Keggin-type structure. Isobutane can be produced from bioethanol in a two-step process. However this process required harsh reaction conditions and the presence of water in bioethanol leads to deactivate the catalyst. The transformation of isobutane to MAA also required extreme conditions due to the less reactive nature of isobutane.

The decarboxylation of carboxylic acids such as citric acid, aconitic acid and IA to MAA is another interesting route. Among the reported feedstocks, IA attracted wide attention because the technology for the transformation of carbohydrates into IA is already commercialized. Despite the great potential, very few research groups are presently working in this field. The main drawback of this approach is that noble metal-based catalysts and corrosive alkaline base are required to obtain high MAA selectivity. The recent efforts from our research group have developed a noble metal free catalyst but the obtained MAA selectivity is not industrially relevant. Much effort should be devoted to develop an atom-efficient heterogeneous catalyst for the high yield production of MAA.

The technology for the industrial production of ethylbenzene using lignin is not matured although the potential for such a process exists. The selective production of ethylbenzene from lignin is very important because the impurities present in the ethylbenzene can render further transformation to ST and downstream processing can increase the overall production cost. To overcome such limitations, Zhao et al. recently proposed a two-step approach for the high yield production (99.3%) of ethylbenzene from corncob lignin.[192b] However, drastic reaction conditions (higher temperature) was required to achieve high ethylbenzene yield.

The oxidative dehydrogenation of ethylbenzene to ST is performed over vanadium, mixed oxides and carbon based catalysts. Recent advances in the catalytic science enabled improved ST selectivity and catalyst stability; however, the catalyst deactivation by coke formation remains a major challenge.

The binary mixed oxide catalyst exhibits excellent catalytic activity compared to those of individual oxides. This is due to their high surface are and acid-base properties that promotes the dehydrogenation of ethylbenzene to ST. The addition of promoters such as Na, K_2O and Ce modified the structure of mixed oxide catalysts and improved the stability.

Moreover, the activity of mixed oxide catalyst can be enhanced by tuning the number of acidic and basic sites by employing such promoters.

While different carbon-based catalysts exhibits remarkable anti-coking properties, thorough studies on the structure-activity relationship of the catalysts as well as mechanistic insight that causes a reduction in the oxidation state of the active species, resulting in the catalyst deactivation, are necessary to mitigate the catalyst deactivation challenge and improve ST productivity.

Several modifications in the catalytic system have been made to prevent this deactivation. For instance, coating a thin carbon layer on the catalyst surface is an effective way to alleviate catalyst coking. Recently, different mesoporous carbon catalysts have been developed, which exhibited improved catalytic performance as well as anti-coking properties under stream free conditions. Utilization of “coked metal oxides" have recently paved the way for the development of remarkably stable dehydrogenation catalysts under oxygen and stream free conditions.[242]

The monomers reviewed in this article are currently produced from fossil resources. The renewed interest in bio-based monomers for environmental sustainability and future energy security has driven the research efforts to produce such products from renewable alternatives in a very creative way. However, most research efforts to date have followed conventional research approach whereby multi-step processing, expensive separation steps of bio-products and catalysts deactivation in the highly oxygenated chemical environments have challenged forecast of minimum selling prices of the derived products to their petroleum analogues. Thus, a holistic approach is necessary to mitigate such challenges. This approach should include the development of stable and multifunctional catalysts for tandem reaction to enable multi-step processing in fewer steps and reactive separation of products without involving cost-intensive separation steps requiring high CapEx and equipment for drop-in replacement bio-products, and design of new functional advantaged monomers for biodegradable plastics. The catalytic approaches should also focus on selectivity and yield improvement of desired monomers to mitigate separation challenges.

Another challenge for bio-refinery is the lack of an established and reliable supply chain for feedstocks, which has been developed for petroleum-based refinery over the last many decades. Development of a similar supply chain for the bio-refinery will require time, and also unparallel investment commitment from public private entities. Such investment should prioritize establishment of upstream bio-based feedstock supply chain, e.g., non-food biomass based sugars and others that are immediate feedstock for vinyl monomers and other

bio-products. Efforts have been invested in the past decade to commercialize such feedstock for downstream bio-products and bioplastics, but there is a disconnection of this effort in recent years. Because of lack of investment and long term commitment, early stage bio-refineries involved in the commercialization and development of supply chain for bio-based feedstock have creased such efforts recently.

While industries should focus on commercialization and supply chain development, academic research institutes should focus on scientific advancement. For example, mechanistic understanding of complex catalytic or biotransformation is not well established for many bio-products syntheses including bio-based vinyl monomers. The academic institute should work hand-on-hand with industries to mitigate industrial challenges. This effort could include more in situ experiment set up to detect real-time catalysts characterization and product formation in complex oxygenated environment involving catalytic sites mobility and delocalization. Incorporation of new catalysis science, e.g. single-atom and duped catalysis should be encouraged.

Another challenge is the lack of techno-economic and life-cycle analysis. While many research groups have randomly chosen bio-products synthesis, more cohesive approach including techno-economic and life-cycle analyses are necessary to guide future direction based on commercial viability and environmental impact of such bio-products and bioplastics. We believe this review article will be useful to a broad research community in academic institutes, industries and policymakers.

Acknowledgements

KA, AB, MG and BL gratefully acknowledge the financial support of the Slovenian Research Agency (ARRS) through the Program P2-0152 and N2-0075. BS acknowledges the financial support from the U. S. Department of Energy, Office of Science, under award number DE-SC0018789.

Abbreviations

IA	Itaconic acid
AA	Acrylic acid
3-HPA	3-Hydroxypropionic acid
LA	Lactic acid
MAA	Methacrylic acid
MMA	Methyl methacrylate
ST	Styrene

References

1. B. M. Upton and A. M. Kasko, *Chem. Rev.*, 2016, **116**, 2275-2306.
2. L. Lebreton and A. Andrady, *Palgrave Commun.,*, 2019, **5**, 6.
3. A. Deneyer, E. Peeters, T. Renders, S. Van den Bosch, N. Van Oeckel, T. Ennaert, T. Szarvas, T. I. Korányi, M. Dusselier and B. F. Sels, *Nat. Energy,*2018, **3**, 969-977.
4. A. Bohre, B. Saha and M. M. Abu-Omar, *ChemSusChem*, 2015, **8**, 4022-4029.
5. L. T. Mika, E. Csefalvay and A. Nemeth, *Chem. Rev.*, 2017, **118**, 505-613.
6. S. Lambert and M. Wagner, *Chem. Soc. Rev.*, 2017, **46**, 6855-6871.
7. S. Molina-Gutiérrez, V. Ladmiral, R. Bongiovanni, S. Caillol and P. Lacroix-Desmazes, *Green Chem.,* 2019, **21**, 36-53.
8. Y. Zhu, C. Romain and C. K. Williams, *Nature*, 2016, **540**, 354.
9. H. Karan, C. Funk, M. Grabert, M. Oey and B. Hankamer, *Trends Plant Sci.,* 2019.
10. V. S. Sikarwar, M. Zhao, P. Clough, J. Yao, X. Zhong, M. Z. Memon, N. Shah, E. J. Anthony and P. S. Fennell, *Energy Environ. Sci.,* 2016, **9**, 2939-2977.
11. A. Bohre, S. Dutta, B. Saha and M. M. Abu-Omar, *ACS Sustain. Chem. Eng.,* 2015, **3**, 1263-1277.
12. M. N. Collins, M. Nechifor, F. Tanasă, M. Zănoagă, A. McLoughlin, M. A. Stróżyk, M. Culebras and C.-A. Teacă, *Int. J. Biol. Macromol.*, 2019, **131**, 828-849.
13. A. Morschbacker, *Polymer Reviews*, 2009, **49**, 79-84.
14. S. Dutta, A. Bohre, W. Zheng, G. R. Jenness, M. Núñez, B. Saha and D. G. Vlachos, *ACS Catal.,* 2017, **7**, 3905-3915.
15. A. Z. Yu, E. M. Serum, A. C. Renner, J. M. Sahouani, M. P. Sibi and D. C. Webster, *ACS Sustain. Chem. Eng.,* 2018, **6**, 12586-12592.
16. K. Satoh, *Polym. J.*, 2015, **47**, 527-536.
17. S. Y. Lee, H. U. Kim, T. U. Chae, J. S. Cho, J. W. Kim, J. H. Shin, D. I. Kim, Y.-S. Ko, W. D. Jang and Y.-S. Jang, *Nat.Catal.*, 2019, **2**, 18-33.
18. R. Beerthuis, G. Rothenberg and N. R. Shiju, *Green Chem.,* 2015, **17**, 1341-1361.
19. I. Delidovich, P. J. C. Hausoul, L. Deng, R. Pfützenreuter, M. Rose and R. Palkovits, *Chem. Rev.*, 2016, **116**, 1540-1599.
20. A. Pellis, E. Herrero Acero, L. Gardossi, V. Ferrario and G. M. Guebitz, *Polym. Int.*, 2016, **65**, 861-871.
21. R. De Clercq, M. Dusselier and B. F. Sels, *Green Chem.,* 2017, **19**, 5012-5040.
22. H. Nakajima, P. Dijkstra and K. Loos, *Polymers*, 2017, **9**, 523.
23. Y. Lee, E. E. Kwon and J. Lee, *Rev Environ Sci Bio.,* 2019, **18**, 317-334.

24. S. Gao, G. Tang, D. Hua, R. Xiong, J. Han, S. Jiang, Q. Zhang and C. Huang, *J. Mater. Chem. B*, 2019, **7**, 709-729.
25. (a) Hirsa M. Torres Galvis, Krijn P. de Jong , *ACS Catal.* 2013*,* **3,** 2130-2149. (b) Yunfei Gao, Luke Neal, Dong Ding, Wei Wu, Chinmoy Baroi, Anne M. Gaffney, and Fanxing Li, *ACS Catal*. 2019, **9**, 8592-8621 (c) A. V. Lavrenov , L. F. Saifulina , E. A. Buluchevskii, E. N. Bogdanets, Catal. Ind., 2015, 7(3), 175-187.
26. L. M. Heidbreder, I. Bablok, S. Drews and C. Menzel, *Sci. Total Environ.*, 2019, **668**, 1077-1093.
27. E. V. Makshina, J. Canadell, J. van Krieken, E. Peeters, M. Dusselier and B. F. Sels, *ChemCatChem*, 2019, **11**, 180-201.
28. M. J. Darabi Mahboub, J.-L. Dubois, F. Cavani, M. Rostamizadeh and G. S. Patience, *Chem. Soc. Rev.*, 2018, **47**, 7703-7738.
29. I. Kainthla, J. T. Bhanushali, R. S. Keri and B. M. Nagaraja, *Catal. Sci. Technol.*, 2015, **5**, 5062-5076.
30. A. J. J. Straathof, S. Sie, T. T. Franco and L. A. M. van der Wielen, *Appl. Microbiol. Biotechnol.*, 2005, **67**, 727-734.
31. D. Sun, Y. Yamada, S. Sato and W. Ueda, *Green Chem.,* 2017, **19**, 3186-3213.
32. H. S. Chu, J.-H. Ahn, J. Yun, I. S. Choi, T.-W. Nam and K. M. Cho, *Metab. Eng.*, 2015, **32**, 23-29.
33. M. A. Droesbeke and F. E. Du Prez, *ACS Sustain. Chem. Eng.,* 2019.
34. X. Wang, H. Wang and Y. Sun, *Chem*, 2017, **3**, 211-228.
35. A. Prieto, M. Palomino, U. Díaz and A. Corma, *Appl. Catal.A,* 2016, **523**, 73-84.
36. P. Sudarsanam, E. Peeters, E. V. Makshina, V. I. Parvulescu and B. F. Sels, *Chem. Soc. Rev.*, 2019, **48**, 2366-2421.
37. S. Veluturla, N. Archna, D. Subba Rao, N. Hezil, I. S. Indraja and S. Spoorthi, *Biofuels*, 2018, **9**, 305-314.
38. H. W. Tan, A. R. Abdul Aziz and M. K. Aroua, *Renew. Sustain. Energy Rev.,* 2013, **27**, 118-127.
39. P. Sudarsanam, R. Zhong, S. Van den Bosch, S. M. Coman, V. I. Parvulescu and B. F. Sels, *Chem. Soc. Rev.*, 2018, **47**, 8349-8402.
40. G. Bagnato, A. Iulianelli, A. Sanna and A. Basile, *Membranes*, 2017, **7**, 17.
41. X. Li and Y. Zhang, *ACS Catal.,* 2016, **6**, 143-150.
42. A. Chieregato, F. Basile, P. Concepción, S. Guidetti, G. Liosi, M. D. Soriano, C. Trevisanut, F. Cavani and J. M. L. Nieto, *Catal. Today*, 2012, **197**, 58-65.

43. K. Omata, K. Matsumoto, T. Murayama and W. Ueda, *Catal. Today*, 2016, **259**, 205-212.
44. Y. Wu, X. Ye, X. Yang, X. Wang, W. Chu and Y. Hu, *Ind. Eng. Chem. Res.*, 1996, **35**, 2546-2560.
45. S. Thanasilp, J. W. Schwank, V. Meeyoo, S. Pengpanich and M. Hunsom, *Chem. Eng. J.*, 2015, **275**, 113-124.
46. X. Li and Y. Zhang, *ACS Catal.,* 2016, **6**, 2785-2791.
47. R. Kappera, D. Voiry, S. E. Yalcin, B. Branch, G. Gupta, A. D. Mohite and M. Chhowalla, *Nature Materials*, 2014, **13**, 1128-1134.
48. L. G. Possato, W. H. Cassinelli, T. Garetto, S. H. Pulcinelli, C. V. Santilli and L. Martins, *Appl. Catal. A,* 2015, **492**, 243-251.
49. B. Sarkar, C. Pendem, L. N. Sivakumar Konathala, R. Tiwari, T. Sasaki and R. Bal, *Chem. Commun.*, 2014, **50**, 9707-9710.
50. M. M. Diallo, J. Mijoin, S. Laforge and Y. Pouilloux, *Catal. Commun.*, 2016, **79**, 58-62.
51. M. B. dos Santos, H. M. C. Andrade and A. J. S. Mascarenhas, *Microporous Mesoporous Mater.*, 2019, **278**, 366-377.
52. I. Eş, A. M. Khaneghah, F. J. Barba, J. A. Saraiva, A. S. Sant'Ana and S. M. B. Hashemi, *Food Res. Int.,* 2018, **107**, 763-770.
53. S. N. Khalifah, Z. N. aini, E. K. Hayati, N. Aini and A. Prasetyo, *IOP Conference Series: Materials Science and Engineering*, 2018, **333**, 012005.
54. G. M. Lari, B. Puértolas, M. S. Frei, C. Mondelli and J. Pérez-Ramírez, *ChemCatChem*, 2016, **8**, 1507-1514.
55. G. Näfe, M. A. López-Martínez, M. Dyballa, M. Hunger, Y. Traa, T. Hirth and E. Klemm, *J. Catal.*, 2015, **329**, 413-424.
56. H. Wang, D. Yu, P. Sun, J. Yan, Y. Wang and H. Huang, *Catal. Commun.*, 2008, **9**, 1799-1803.
57. J. Zhang, Y. Zhao, M. Pan, X. Feng, W. Ji and C.-T. Au, *ACS Catal.,* 2011, **1**, 32-41.
58. J. Zhang, Y. Zhao, X. Feng, M. Pan, J. Zhao, W. Ji and C.-T. Au, *Catal. Sci. Technol.*, 2014, **4**, 1376-1385.
59. P. Sun, D. Yu, K. Fu, M. Gu, Y. Wang, H. Huang and H. Ying, *Catal. Commun.*, 2009, **10**, 1345-1349.
60. P. Sun, D. Yu, Z. Tang, H. Li and H. Huang, *Ind. Eng. Chem. Res.*, 2010, **49**, 9082-9087.

61. L. Zhang, D. S. Theng, Y. Du, S. Xi, L. Huang, F. Gao, C. Wang, L. Chen and A. Borgna, *Catal. Sci. Technol.*, 2017, **7**, 6101-6111.
62. J. Z. S. Zuo, J. Liu, *CN 102019193.*, 2011.
63. B. Yan, A. Mahmood, Y. Liang and B.-Q. Xu, *Catal. Today*, 2016, **269**, 65-73.
64. B. Yan, L.-Z. Tao, Y. Liang and B.-Q. Xu, *ChemSusChem*, 2014, **7**, 1568-1578.
65. C. Yuan, H. Liu, Z. Zhang, H. Lu, Q. Zhu and Y. Chen, *Chinese J. Catal.*, 2015, **36**, 1861-1866.
66. X. Zhang, L. Lin, T. Zhang, H. Liu and X. Zhang, *Chem. Eng. J.*, 2016, **284**, 934-941.
67. Q. L. B. Jiang, D. Li, W. Wang, , 2009, **CN 101602010**.
68. X. Z. X. Zhang, Y. Dong, H. Liu, 2015, **CN 104399515.**
69. R. E. Holmen, *US2859240A,* 1958.
70. V. C. Ghantani, S. T. Lomate, M. K. Dongare and S. B. Umbarkar, *Green Chem.,* 2013, **15**, 1211-1217.
71. Y. Matsuura, A. Onda, S. Ogo and K. Yanagisawa, *Catal. Today*, 2014, **226**, 192-197.
72. Y. Matsuura, A. Onda and K. Yanagisawa, *Catal. Commun.*, 2014, **48**, 5-10.
73. E. Blanco, P. Delichere, J. M. M. Millet and S. Loridant, *Catal. Today*, 2014, **226**, 185-191.
74. B. Yan, L.-Z. Tao, Y. Liang and B.-Q. Xu, *ACS Catal.,* 2014, **4**, 1931-1943.
75. S. B. U. M. K. Dongare, S. Lomate, 2012, **WO 2012/156921**.
76. Y. M. A. Onda, K. Yanagisawa, J. Kubo, 2016, , **US 2016/0096166**.
77. V. C. Ghantani, M. K. Dongare and S. B. Umbarkar, *RSC Adv.,* 2014, **4**, 33319-33326.
78. C. Tang, J. Peng, X. Li, Z. Zhai, N. Jiang, W. Bai, H. Gao and Y. Liao, *RSC Adv.,* 2014, **4**, 28875-28882.
79. C. Tang, J. Peng, G. Fan, X. Li, X. Pu and W. Bai, *Catal. Commun.*, 2014, **43**, 231-234.
80. D. I. C. J. V. Lingoes, 2013, **US 2013/0274514.**
81. J. V. L. J. E. Velasquez, J. E. Godlewski, D. I. Collias, F. C. Wireko, M. A. Mamak, N. L. Redman-Furey, 2013, **WO 2013/155270**.
82. Z. Guo, D. S. Theng, K. Y. Tang, L. Zhang, L. Huang, A. Borgna and C. Wang, *PCCP*, 2016, **18**, 23746-23754.
83. N. Nagaraju, V. P. Kumar, A. Srikanth, N. P. Rajan and K. V. R. Chary, *Appl. Petrochem. Res.,* 2016, **6**, 367-377.
84. D. T. Vu, A. K. Kolah, N. S. Asthana, L. Peereboom, C. T. Lira and D. J. Miller, *Fluid Phase Equilib.*, 2005, **236**, 125-135.

85. J. Zhang, J. Lin and P. Cen, *Can J Chem Eng.,* 2008, **86**, 1047-1053.
86. G. C. Gunter, R. H. Langford, J. E. Jackson and D. J. Miller, *Ind. Eng. Chem. Res.*, 1995, **34**, 974-980.
87. M. Stalpaert, N. Peeters and D. De Vos, *Catal. Sci. Technol.*, 2018, **8**, 1468-1474.
88. I. P. Rosas, J. L. C. Larios, B. Zeifert and J. S. Blásquez, in *Glycerine Production and Transformation-An Innovative Platform for Sustainable Biorefinery and Energy*, IntechOpen, 2019.
89. A. Corma, G. W. Huber, L. Sauvanaud, P. O'Connor, *J. catal.,*, 2008, **257**, 163-171.
90. S. Ishikawa, X. Yi, T. Murayama and W. Ueda, *Catal. Today*, 2014, **238**, 35-40.
91. C. Chen, N. Kosuke, T. Murayama and W. Ueda, *ChemCatChem*, 2013, **5**, 2869-2873.
92. T. Fjermestad, W.-q. Li, G. Rugg, S. Ishida, M. Okuno, K. Sagi, A. Genest and N. Rösch, *Appl. Catal. A,* 2018, **565**, 68-75.
93. J. Kunert, A. Drochner, J. Ott, H. Vogel and H. Fueß, *Appl. Catal. A,* 2004, **269**, 53-61.
94. S. Ishikawa and W. Ueda, *Catal. Sci. Technol.*, 2016, **6**, 617-629.
95. A. H. Adams, F. Haaß, T. Buhrmester, J. Kunert, J. Ott, H. Vogel and H. Fuess, *J. Mol. Catal. A: Chem.*, 2004, **216**, 67-74.
96. P. Kampe, L. Giebeler, D. Samuelis, J. Kunert, A. Drochner, F. Haaß, A. H. Adams, J. Ott, S. Endres, G. Schimanke, T. Buhrmester, M. Martin, H. Fuess and H. Vogel, *PCCP*, 2007, **9**, 3577-3589.
97. P. Jakes, N. Blickhan, T. Jekewitz, A. Drochner, H. Vogel, H. Fuess and R.-A. Eichel, *ChemPhysChem*, 2011, **12**, 3578-3583.
98. A. Drochner, P. Kampe, N. Menning, N. Blickhan, T. Jekewitz and H. Vogel, *Chem. Eng. Tech.*, 2014, **37**, 398-408.
99. Li, Wen-Qing, Fjermestad, Torstein, Genest, Alexander, Rösch, Notker, Cat. Sci. Technol., 2019, 9, 1559-1569.
100. H. Werner, O. Timpe, D. Herein, Y. Uchida, N. Pfänder, U. Wild, R. Schlögl and H. Hibst, *Catal. Lett.*, 1997, **44**, 153-163.
101. S. Endres, P. Kampe, J. Kunert, A. Drochner and H. Vogel, *Appl. Catal. A,* 2007, **325**, 237-243.
102. A. S. L. Thankamony, S. Knoche, S. Bothe, A. Drochner, A. P. Jagtap, S. T. Sigurdsson, H. Vogel, B. J. M. Etzold, T. Gutmann and G. Buntkowsky, *J. Phys. Chem. C*, 2017, **121**, 20857-20864.

103. S. Erfle, U. Armbruster, U. Bentrup, A. Martin and A. Brückner, *Appl. Catal. A,* 2011, **391**, 102-109.
104. A. Dinse, A. Ozarowski, C. Hess, R. Schomäcker and K.-P. Dinse, *J. Phys. Chem. C*, 2008, **112**, 17664-17671.
105. Y. Uchida, G. Mestl, O. Ovsitser, J. Jäger, A. Blume and R. Schlögl, *J. Mol. Catal. A: Chem.*, 2002, **187**, 247-257.
106. C.-R. Chang, Z.-Q. Huang and J. Li, *WIREs Computational Molecular Science*, 2016, **6**, 679-693.
107. T. Jekewitz, N. Blickhan, S. Endres, A. Drochner and H. Vogel, *Catal. Commun.*, 2012, **20**, 25-28.
108. T. Petzold, N. Blickhan, A. Drochner and H. Vogel, *ChemCatChem*, 2014, **6**, 2053-2058.
109. S. Ishikawa, Y. Goto, Y. Kawahara, S. Inukai, N. Hiyoshi, N. F. Dummer, T. Murayama, A. Yoshida, M. Sadakane and W. Ueda, *Chem. Mater.*, 2017, **29**, 2939-2950.
110. S. Ishikawa, Y. Yamada, C. Qiu, Y. Kawahara, N. Hiyoshi, A. Yoshida and W. Ueda, *Chem. Mater.*, 2019, **31**, 1408-1417.
111. P. Botella, B. Solsona, A. Martinez-Arias and J. M. López Nieto, *Catal. Lett.*, 2001, **74**, 149-154.
112. S. Ishikawa, T. Murayama, B. Katryniok, F. Dumeignil, M. Araque, S. Heyte, S. Paul, Y. Yamada, M. Iwazaki and N. Noda, *Appl. Catal. A,* 2019, **584**, 117151.
113. S. Ishikawa, T. Murayama, B. Katryniok, F. Dumeignil, M. Araque, S. Heyte, S. Paul, Y. Yamada, M. Iwazaki, N. Noda and W. Ueda, *Appl. Catal. A,* 2019, **584**, 117151.
114. B. Frank, R. Blume, A. Rinaldi, A. Trunschke and R. Schlögl, 2011.
115. B. Frank, R. Blume, A. Rinaldi, A. Trunschke and R. Schlögl, *Angew. Chem. Int. Ed.*, 2011, **50**, 10226-10230.
116. B. Zhong, H. Liu, X. Gu and D. S. Su, *ChemCatChem*, 2014, **6**, 1553-1557.
117. B. Zhong, R. Huang, D. S. Su and H. Liu, *Catal. Today*, 2019, **330**, 142-148.
118. L. Matsakas, K. Hrůzová, U. Rova and P. Christakopoulos, *Fermentation*, 2018, **4**, 13.
119. T. Dishisha, S.-H. Pyo and R. Hatti-Kaul, *Microb.Cell Factor.*, 2015, **14**, 200.
120. L. Craciun, G. P. Benn, J. Dewing, G. W. Schriver, W. J. Peer, B. Siebenhaar and U. Siegrist, *US 20050222458A1*, 2009.
121. J. F. W. M. A. Lilga, J. E. Holladay, A. H. Zacher, D. S. Muzatko, R. J. Orth, 2007, US 2007/0219391.

122. A. H. Z. J. E. Holladay, M. A. Lilga, J. F. White, D. S. Muzatko, R. J. Orth, P. Tsobanakis, X. Meng, T. W. Abraham, 2007, WO 2007/106099.
123. N. H. H. Kamei, H. Yoshida, 2014, *JP 2014009168*.
124. C. Li, Q. Zhu, Z. Cui, B. Wang, Y. Fang and T. Tan, *Chem. Eng. Sci.*, 2018, **183**, 288-294.
125. D. D. R. Tengler, S. Hoyt, S. Roach, , 2013, *WO 2013/192453*, 2013.
126. N. S. P. 26J. Chwae, M. H. Lee, J. W. Kim, *US 2014/0171681*, 2014.
127. T. Murayama, B. Katryniok, S. Heyte, M. Araque, S. Ishikawa, F. Dumeignil, S. Paul and W. Ueda, *ChemCatChem*, 2016, **8**, 2415-2420.
128. S. Yang, M. Kim, S. Yang, D. S. Kim, W. J. Lee and H. Lee, *Catal. Sci. Technol.*, 2016, **6**, 3616-3622.
129. M. Kim and H. Lee, *ChemistrySelect*, 2017, **2**, 2420-2425.
130. M. Kim and H. Lee, *ACS Sustain. Chem. Eng.,* 2017, **5**, 11371-11376.
131. A. Vidra and Á. Németh, *Periodica Polytechnica Chemical Engineering*, 2018, **62**, 245-256.
132. J.-W. Bae, H. S. Potdar, S.-H. Kang and K.-W. Jun, *Energy & Fuels*, 2008, **22**, 223-230.
133. J. F. Vitcha and V. A. Sims, *I&EC Product Research and Development*, 1966, **5**, 50-53.
134. A.-n. Parvulescu, A. L. De Oliveira, M. Lejkowski, N. T. Woerz, M. Hartmann, K. Amakawa, M. Goebel, U. Mueller, M. Feyen and Y. Liu, *US8507721B2,* 2016.
135. J. Hu, Z. Lu, H. Yin, W. Xue, A. Wang, L. Shen and S. Liu, *J. Ind. Eng. Chem.*, 2016, **40**, 145-151.
136. J. Liu, P. Xu, P. Wang, Z. Xu, X. Feng, W. Ji and C.-T. Au, *Sci. Rep.*, 2019, **9**, 16988.
137. D. Yang, C. Sararuk, K. Suzuki, Z. Li and C. Li, *Chem. Eng. J.*, 2016, **300**, 160-168.
138. M. Ai, *J. Catal.*, 1987, **107**, 201-208.
139. X. Feng, B. Sun, Y. Yao, Q. Su, W. Ji and C.-T. Au, *J. Catal.*, 2014, **314**, 132-141.
140. F. Wang, J.-L. Dubois and W. Ueda, *J. Catal.*, 2009, **268**, 260-267.
141. D. Yang, D. Li, H. Yao, G. Zhang, T. Jiao, Z. Li, C. Li and S. Zhang, *Ind. Eng. Chem. Res.*, 2015, **54**, 6865-6873.
142. E. M. Karp, T. R. Eaton, V. Sànchez i Nogué, V. Vorotnikov, M. J. Biddy, E. C. D. Tan, D. G. Brandner, R. M. Cywar, R. Liu, L. P. Manker, W. E. Michener, M. Gilhespy, Z. Skoufa, M. J. Watson, O. S. Fruchey, D. R. Vardon, R. T. Gill, A. D. Bratis and G. T. Beckham, *Science*, 2017, **358**, 1307-1310.

143. U. Ali, K. J. B. A. Karim and N. A. Buang, *Polym. Rev.,* 2015, **55**, 678-705.
144. K. Nagai, *Appl. Catal. A,*2001, **221**, 367-377.
145. N. Mizuno and H. Yahiro, *J. Phys. Chem. B*, 1998, **102**, 437-443.
146. K. Kida, *EP 094198 4A3*, 1999.
147. H. Higuchi and K. Kida, 1991, EP2003114A1.
148. J. Gao, G. Fan, L. Yang, X. Cao, P. Zhang and F. Li, *ChemCatChem*, 2017, **9**, 1230-1241.
149. B. Li, R. Yan, L. Wang, Y. Diao, Z. Li and S. Zhang, *Catal. Lett.*, 2013, **143**, 829-838.
150. B. N. van Leeuwen, A. M. van der Wulp, I. Duijnstee, A. J. van Maris and A. J. Straathof, *Appl. Microbiol. Biotechnol.*, 2012, **93**, 1377-1387.
151. S. Paul, W. Chu, M. Sultan and E. Bordes-Richard, *Sci. China Chem.*, 2010, **53**, 2039-2046.
152. W. Li and W. Ueda, *Catal. Lett.*, 1997, **46**, 261-265.
153. N. Mizuno, M. Tateishi and M. Iwamoto, *J. Chem. Soc., Chem. Commun.*, 1994, 1411-1412.
154. N. Mizuno, M. Tateishi and M. Iwamoto, *J. Catal.*, 1996, **163**, 87-94.
155. M. Langpape and J.-M. M. Millet, *Appl. Catal. A,* 2000, **200**, 89-101.
156. J.-S. Min and N. Mizuno, *Catal. Today*, 2001, **71**, 89-96.
157. F. Cavani, R. Mezzogori, A. Pigamo and F. Trifirò, *Comptes Rendus de l'Académie des Sciences - Series IIC - Chemistry*, 2000, **3**, 523-531.
158. M. Sultan, S. Paul, M. Fournier and D. Vanhove, *Appl. Catal. A,*2004, **259**, 141-152.
159. (a) S. Wu, Q. Kan, W. Ding, F. Shang, H. Liu and J. Guan, *React Kinet Mech Cat.,* 2012, **106**, 157-164. (b) Feng Xian Liu-Caia, Charlotte Phamb, Farida Beya and Gilbert Herve, *React Kinet Catal. Lett.,* 2002, **75(2),** 305-314.
160. J. He, Y. Liu, W. Chu and W. Yang, *Appl. Catal. A,* 2018, **556**, 104-112.
161. F. Jing, B. Katryniok, E. Bordes-Richard and S. Paul, *Catal. Today*, 2013, **203**, 32-39.
162. F. Jing, B. Katryniok, F. Dumeignil, E. Bordes-Richard and S. Paul, *J. Catal.*, 2014, **309**, 121-135.
163. F. Jing, B. Katryniok, F. Dumeignil, E. Bordes-Richard and S. Paul, *Catal. Sci. Technol.*, 2014, **4**, 2938-2945.
164. J.-S. Min and N. Mizuno, *Catal. Today*, 2001, **66**, 47-52.
165. N. Mizuno, D.-J. Suh, W. Han and T. Kudo, *J. Mol. Catal. A: Chem.*, 1996, **114**, 309-317.

166. G. Mestl, T. Ilkenhans, D. Spielbauer, M. Dieterle, O. Timpe, J. Kröhnert, F. Jentoft, H. Knözinger and R. Schlögl, *Appl. Catal. A,*2001, **210**, 13-34.
167. E. Etienne, F. Cavani, R. Mezzogori, F. Trifirò, G. Calestani, L. Gengembre and M. Guelton, *Appl. Catal. A,* 2003, **256**, 275-290.
168. G. Busca, F. Cavani, E. Etienne, E. Finocchio, A. Galli, G. Selleri and F. Trifirò, *J. Mol. Catal. A: Chem.*, 1996, **114**, 343-359.
169. N. Mizuno, W. Han and T. Kudo, *J. Catal.*, 1998, **178**, 391-394.
170. Y. Liu, J. He, W. Chu and W. Yang, *Catal. Sci. Technol.*, 2018, **8**, 5774-5781.
171. Y. Zheng, H. Zhang, L. Wang, S. Zhang and S. Wang, *Front Chem Sci Eng.,* 2016, **10**, 139-146.
172. J. Guan, H. Wang, K. Song, C. Xu, Z. Wang and Q. Kan, *Catal. Commun.*, 2009, **10**, 1437-1440.
173. J. Guan, S. Wu, H. Wang, S. Jing, G. Wang, K. Zhen and Q. Kan, *J. Catal.*, 2007, **251**, 354-362.
174. J. H. Yeap, *Catalytic Upgrading of Biomass-Derived Carboxylic Acids to Fuels and Chemicals*, EPFL, 2019.
175. M. Carlsson, C. Habenicht, L. C. Kam, M. J. Antal, Jr., N. Bian, R. J. Cunningham and M. Jones, Jr., *Ind. Eng. Chem. Res.*, 1994, **33**, 1989-1996.
176. D. W. Johnson, G. R. Eastham, M. Poliakoff and T. A. Huddle, *Journal*, 2015.
177. J. Li, T.B. Brill, *J. Phys. Chem. A*., 2001, **105**, 10839–10845.
178. J. C. Lansing, R. E. Murray and B. R. Moser, *ACS Sustain. Chem. Eng.,* 2017, **5**, 3132-3140.
179. J. Le Nôtre, S. C. M. Witte-van Dijk, J. van Haveren, E. L. Scott and J. P. M. Sanders, *ChemSusChem*, 2014, **7**, 2712-2720.
180. M. Pirmoradi and J. R. Kastner, *ACS Sustain. Chem. Eng.,* 2017, **5**, 1517-1527.
181. T. Rohwerder and R. H. Müller, *Microb. Cell Fact.,* 2010, **9**, 13.
182. A. Bohre, B. Hočevar, M. Grilc and B. Likozar, *Appl. Catal. B,* 2019, **256**, 117889.
183. J. Gao, C. Jia, M. Zhang, F. Gu, G. Xu, Z. Zhong and F. Su, *RSC Adv.,* 2013, **3**, 18156-18163.
184. A. Bohre, M. A. Ali, M. Ocepek, M. Grilc, J. Zabret and B. Likozar, *Ind. Eng. Chem. Res.*, 2019, **58**, 19825-19831.
185. M. Jaymand, *Polym. Chem.,*2014, **5**, 2663-2690.
186. J. Lian, R. McKenna, M. R. Rover, D. R. Nielsen, Z. Wen and L. R. Jarboe, *J. Ind. Microbiol. Biotechnol.* 2016, **43**, 595-604.

187. N. Chaukura, W. Gwenzi, T. Bunhu, D. T. Ruziwa and I. Pumure, *Resour Conserv Recy.,* 2016, **107**, 157-165.
188. T. R. Carlson, G. A. Tompsett, W. C. Conner and G. W. Huber, *Top. Catal.*, 2009, **52**, 241.
189. R. Rinaldi, R. Jastrzebski, M. T. Clough, J. Ralph, M. Kennema, P. C. Bruijnincx and B. M. Weckhuysen, *Angew. Chem. Int. Ed.*, 2016, **55**, 8164-8215.
190. W. Schutyser, T. Renders, S. Van den Bosch, S.-F. Koelewijn, G. Beckham and B. F. Sels, *Chem. Soc. Rev.*, 2018, **47**, 852-908.
191. M. Fan, P. Jiang, P. Bi, S. Deng, L. Yan, Q. Zhai, T. Wang and Q. Li, *Bioresour. Technol.*, 2013, **143**, 59-67.
192. (a) A. Wang and H. Song, *Bioresour. Technol.*, 2018, **268**, 505-513; (b) Z. Luo, S. Qin, S. Chen, Y. Hui and C. Zhao, *Green Chem*., 2020, **22,** 1842-1850. (c) L. Li, Lin Dong, X. Liu, Y. Guo, Y. Wang, *Appl.Catal. B*,2020, **260**, 118143.
193. P. N. Degannes and D. M. Ruthven, *Can J Chem Eng.,* 1979, **57**, 627-630.
194. M.-o. Sugino, H. Shimada, T. Turuda, H. Miura, N. Ikenaga and T. Suzuki, *Appl. Catal. A,* 1995, **121**, 125-137.
195. D. Mukherjee, S.-E. Park and B. M. Reddy, *J. CO_2 Util.*, 2016, **16**, 301-312.
196. A. Burri, N. Jiang, K. Yahyaoui and S.-E. Park, *Appl. Catal. A,* 2015, **495**, 192-199.
197. M. O. Guerrero-Pérez, *Catal. Today*, 2017, **285**, 226-233.
198. M. O. Guerrero-Pérez, *Catalysts*, 2018, **8**, 564.
199. A. Sun, Z. Qin, S. Chen and J. Wang, *J. Mol. Catal. A: Chem.*, 2004, **210**, 189-195.
200. L. Zhang, Z. Wu, N. C. Nelson, A. D. Sadow, I. I. Slowing and S. H. Overbury, *ACS Catal.*, 2015, **5**, 6426-6435.
201. R. R. Langeslay, D. M. Kaphan, C. L. Marshall, P. C. Stair, A. P. Sattelberger and M. Delferro, *Chem. Rev.*, 2018, **119**, 2128-2191.
202. M. Betiha, A. Rabie, A. Elfadly and F. Yehia, *Micropor. Mesoporor. Mat.*, 2016, **222**, 44-54.
203. C. Zhu, S. Chen, D. Pan, X. Cui, Y. Qiao and R. Li, *Catal. Commun.*, 2018, **115**, 12-16.
204. C. Nederlof, F. Kapteijn and M. Makkee, *Appl. Catal. A,* 2012, **417**, 163-173.
205. I. M. Nogueira, G. Q. Sabadia, A. A. Moreira, M. Josue Filho and A. C. Oliveira, *J. Mol. Catal. A: Chem.*, 2011, **351**, 81-92.
206. T. Wang, S. Chong, T. Wang, H. Lu and M. Ji, *Appl. Surf. Sci.*, 2018, **427**, 1011-1018.

207. I. Kainthla, G. V. R. Babu, J. T. Bhanushali, R. S. Keri, K. S. R. Rao and B. M. Nagaraja, *New J. Chem.*, 2017, **41**, 4173-4181.
208. M. B. Ansari and S.-E. Park, *Energy Environ. Sci.,* 2012, **5**, 9419-9437.
209. N. Jiang, A. Burri and S.-E. Park, *Chinese J. Catal.,* 2016, **37**, 3-15.
210. D. R. Burri, K. M. Choi, D.-S. Han, J.-B. Koo and S.-E. Park, *Catal. Today*, 2006, **115**, 242-247.
211. D. R. Burri, K.-M. Choi, S.-C. Han, A. Burri and S.-E. Park, *J. Mol. Catal. A: Chem.*, 2007, **269**, 58-63.
212. B. M. Reddy, S.-C. Lee, D.-S. Han and S.-E. Park, *Appl. Catal. B,* 2009, **87**, 230-238.
213. D. R. Burri, K.-M. Choi, D.-S. Han, N. Jiang, A. Burri and S.-E. Park, *Catal. Today*, 2008, **131**, 173-178.
214. I. Wang, W.-F. Chang, R.-J. Shiau, J.-C. Wu and C.-S. Chung, *J. Catal.*, 1983, **83**, 428-436.
215. V. R. Madduluri, P. Nagaiah, C. Prathap, K. Vasikerappa, A. Nagu, B. D. Raju and K. S. R. Rao, *Arab. J. Chem.,* 2020, 13(1), 2883-2896.
216. H.-X. Fan, J. Feng, W.-Y. Li, X.-H. Li, T. Wiltowski and Q.-F. Ge, *Appl. Surf. Sci.*, 2018, **427**, 973-980.
217. X. Li, J. Feng, H. Fan, Q. Wang and W. Li, *Catal. Commun.*, 2015, **59**, 104-107.
218. K. N. Rao, B. M. Reddy and S.-E. Park, *Appl. Catal. B,* 2010, **100**, 472-480.
219. D. R. Burri, K.-M. Choi, J.-H. Lee, D.-S. Han and S.-E. Park, *Catal. Commun.*, 2007, **8**, 43-48.
220. Q. Wang, X. Li, W. Li and J. Feng, *Catal. Commun.*, 2014, **50**, 21-24.
221. A. K. Venugopal, A. T. Venugopalan, P. Kaliyappan and T. Raja, *Green Chem.,* 2013, **15**, 3259-3267.
222. C. Nederlof, V. Zarubina, I. Melián-Cabrera, H. J. E. Heeres, F. Kapteijn and M. Makkee, *Catal. Sci. Technol.*, 2013, **3**, 519-526.
223. A. A. Al-Zahrani, N. Pasupulety, M. A. Daous, H. Driss, A. M. Ali, S. F. Zaman and L. A. Petrov, *Appl. Catal. A,* 2018, **552**, 49-57.
224. J. Diao, Y. Zhang, J. Zhang, J. Wang, H. Liu and D. S. Su, *Chem. Commun.*, 2017, **53**, 11322-11325.
225. N. Gupta, Q. Wang, G. Wen, D. Su, 2017, In Micro and Nano Technologies, Nanodiamonds, Elsevier, Chapter 18, , 439-463.
226. V. N. Mochalin, O. Shenderova, D. Ho and Y. Gogotsi, *Nat. Nanotechnol.,* 2012, **7**, 11.

227. G. Grunewald and R. Drago, *J. Mol. Catal.*, 1990, **58**, 227-233.
228. M. F. R. Pereira, J. L. Figueiredo, J. J. Órfão, P. Serp, P. Kalck and Y. Kihn, *Carbon*, 2004, **42**, 2807-2813.
229. J. J. Delgado, X. Chen, J.-P. Tessonnier, M. E. Schuster, E. Del Rio, R. Schlögl and D. S. Su, *Catal. Today*, 2010, **150**, 49-54.
230. L. Qin, L. Wang, C. Wang, X. Yang and B. Lv, *Mol. Catal.*, 2019, **462**, 61-68.
231. P.-X. Hou, C. Liu and H.-M. Cheng, *Carbon*, 2008, **46**, 2003-2025.
232. N. Qui, P. Scholz, T. Krech, T. Keller, K. Pollok and B. Ondruschka, *Catal. Commun.*, 2011, **12**, 464-469.
233. H. Ou, P. Yang, L. Lin, M. Anpo and X. Wang, *Angew. Chem. Int. Ed.*, 2017, **56**, 10905-10910.
234. Y. Lin, X. Sun, D. S. Su, G. Centi and S. Perathoner, *Chem. Soc. Rev.*, 2018, **47**, 8438-8473.
235. J. Zhang, D. S. Su, R. Blume, R. Schlögl, R. Wang, X. Yang and A. Gajović, *Angew. Chem. Int. Ed.*, 2010, **49**, 8640-8644.
236. Z. Zhao and Y. Dai, *J. Mater. Chem. A*, 2014, **2**, 13442-13451.
237. H. Ba, L. Truong-Phuoc, Y. Liu, C. Duong-Viet, J.-M. Nhut, L. Nguyen-Dinh, P. Granger and C. Pham-Huu, *Carbon*, 2016, **96**, 1060-1069.
238. J. Diao, Z. Feng, R. Huang, H. Liu, S. B. A. Hamid and D. S. Su, *ChemSusChem*, 2016, **9**, 662-666.
239. Z. Zhao, W. Li, Y. Dai, G. Ge, X. Guo and G. Wang, *ACS Sustain. Chem. Eng.,* 2015, **3**, 3355-3364.
240. Q. Zhou, X. Guo, C. Song and Z. Zhao, *ACS Appl. Nano Mater.,* 2019, **2**, 2152-2159.
241. L. Feng, Y. Liu, Q. Jiang, W. Liu, K.-H. Wu, H. Ba, C. Pham-Huu, W. Yang and D. S. Su, *Catal. Today*, 2019.
242. H. Ba, G. Tuci, C. Evangelisti, M. Ceppatelli, L. Nguyen-Dinh, V. Dal Santo, F. Bossola, J.-M. Nhut, A. Rossin, P. Granger, G. Giambastiani and C. Pham-Huu, *ACS Catal.,* 2019, **9**, 9474-9484.
243. F. Wang, J. Xu, J. L. Dubois and W. Ueda, *ChemSusChem*, 2010, **3**, 1383-1389.
244. M. D. Soriano, P. Concepción, J. L. Nieto, F. Cavani, S. Guidetti and C. Trevisanut, *Green Chem.* 2011, **13**, 2954-2962.
245. A. Chieregato, M. D. Soriano, F. Basile, G. Liosi, S. Zamora, P. Concepción, F. Cavani and J. M. L. Nieto, *Appl. Catal. B,* 2014, **150**, 37-46.

246. A. Chieregato, M. D. Soriano, E. García-González, G. Puglia, F. Basile, P. Concepción, C. Bandinelli, J. M. López Nieto and F. Cavani, *ChemSusChem*, 2015, **8**, 398-406.

247. Y. S. Yun, K. R. Lee, H. Park, T. Y. Kim, D. Yun, J. W. Han and J. Yi, *ACS Catal.,* 2014, **5**, 82-94.

248. C. F. Pestana, A. C. Guerra, G. B. Ferreira, C. C. Turci and C. J. Mota, *J. Braz. Chem. Soc.,* 2013, **24**, 100-105.

249. L. Liu, B. Wang, Y. Du, Z. Zhong and A. Borgna, *Appl. Catal. B,* 2015, **174**, 1-12.

250. A. S. Paula, L. G. Possato, D. R. Ratero, J. Contro, K. Keinan-Adamsky, R. R. Soares, G. Goobes, L. Martins and J. G. Nery, *Micropor. Mesoporor. Mat.*, 2016, **232**, 151-160.

251. A. Witsuthammakul and T. Sooknoi, *Appl. Catal. A,* 2012, **413**, 109-116.

252. R. Liu, T. Wang, D. Cai and Y. Jin, *Ind. Eng. Chem. Res.*, 2014, **53**, 8667-8674.

253. M. Langpape, J. M. M. Millet, U. S. Ozkan and P. Delichère, *J. Catal.*, 1999, **182**, 148-155.

254. A. Sun, Z. Qin, S. Chen and J. Wang, *Catal. Today*, 2004, **93-95**, 273-279.

255. B. S. Liu, G. Rui, R. Z. Chang and C. T. Au, *Appl. Catal. A,*2008, **335**, 88-94.

256. R. D. Holtz, S. B. d. Oliveira, M. A. Fraga and M. d. C. Rangel, *Appl. Catal. A,* 2008, **350**, 79-85.

257. M.-S. Park, V. P. Vislovskiy, J.-S. Chang, Y.-G. Shul, J. S. Yoo and S.-E. Park, *Catal. Today*, 2003, **87**, 205-212.

258. V. R. B. Gurram, S. S. Enumula, S. Mutyala, R. Pochamoni, P. S. S. Prasad, D. R. Burri and S. R. R. Kamaraju, *Appl. Petrochem. Res.,* 2016, **6**, 427-437.

259. C. Li, C. Miao, Y. Nie, Y. Yue, S. Gu, W. Yang, W. Hua and Z. Gao, *Chinese J. Catal.,* 2010, **31**, 993-998.

260. C. Wang, W.-B. Fan, Z.-T. Liu, J. Lu, Z.-W. Liu, Z.-F. Qin and J.-G. Wang, *J. Mol. Catal. A: Chem.*, 2010, **329**, 64-70.

261. I. Kainthla, G. V. R. Babu, J. T. Bhanushali, K. S. R. Rao and B. M. Nagaraja, *J. CO_2 Util.*, 2017, **18**, 309-317.

262. N. Jiang, D.-S. Han and S.-E. Park, *Catal. Today*, 2009, **141**, 344-348.

263. A. J. R. Castro, S. P. D. Marques, J. M. Soares, J. M. Filho, G. D. Saraiva and A. C. Oliveira, *Chem. Eng. J.*, 2012, **209**, 345-355.

Figures and Schemes caption

Figure 1: Biomass derived vinyl monomers and precursors for the production of acrylic acid, methacrylic acid and styrene: EB = ethylbenzene: ACR = acrolein; ALA = allyl alcohol; IB = isobutylene; IA = itaconic acid; GLY = glycerol and LA = lactic acid.

Figure 2: Acrylic acid production from bio-derived feedstock (green), bio-derived platform chemicals (light blue), and petroleum (grey). Modified with permission from ref. 18, Copyright (2015) Royal Society of Chemistry.

Scheme 1: Two-steps and one-step conversion of glycerol to AA.

Scheme 2: Synthesis of AA from lactic acid over calcium pyrophosphate catalyst.

Scheme 3: Synthesis AA via 3-HPA platform.

Scheme 4: Oxidation of allyl alcohol to AA.

Scheme 5: Synthesis AA by the aldol condensation of acetic acid and formaldehyde.

Scheme 6: Selective oxidation of isobutane to MAA.

Scheme 7: Proposed reaction mechanism for ethylbenzene dehydrogenation to ST over VOx/SiO_2 catalyst in CO_2. Reproduced with permission from ref. 203, Copyright (2018) Elsevier.

Figure 1:

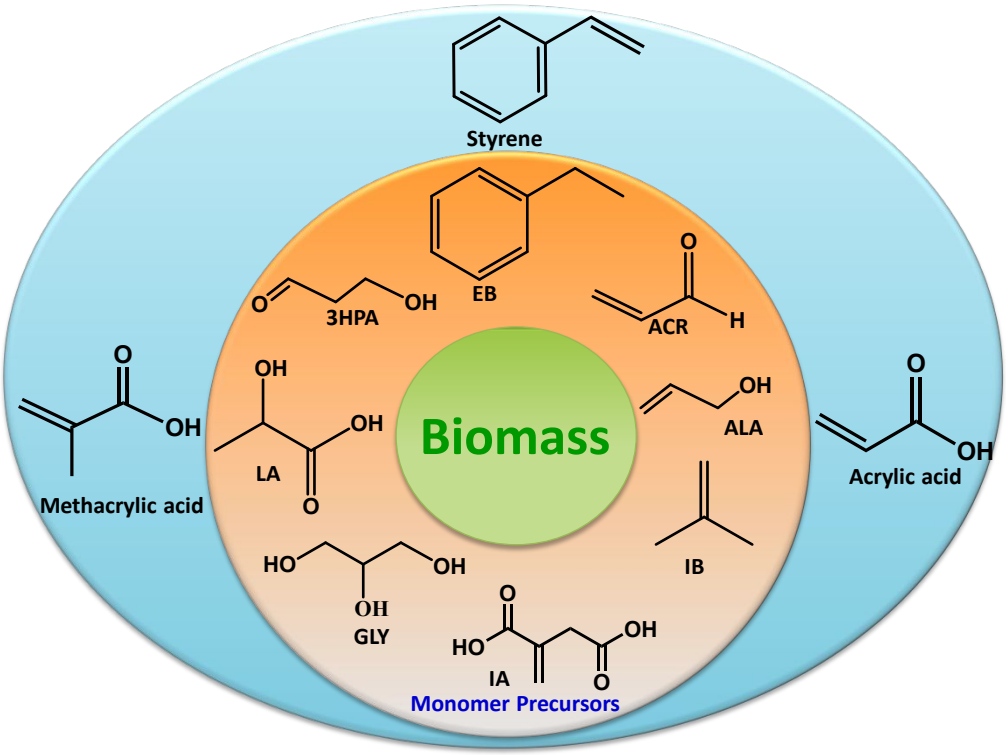

Figure 2:

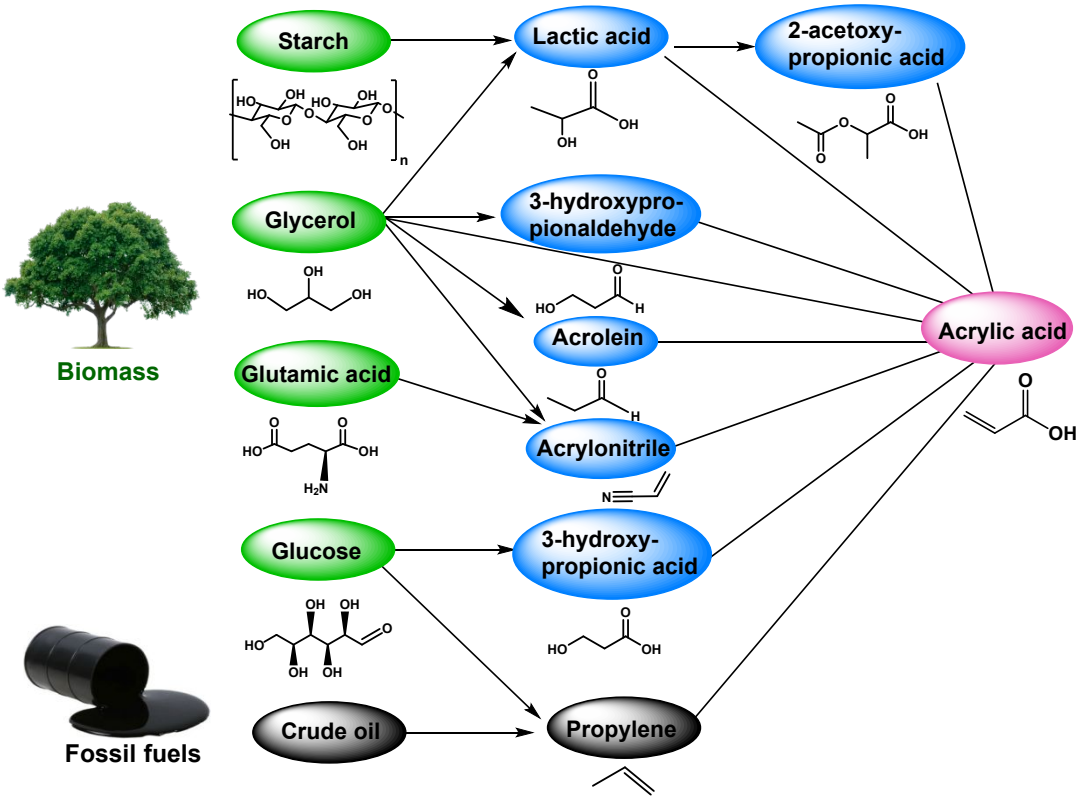

Scheme 1:

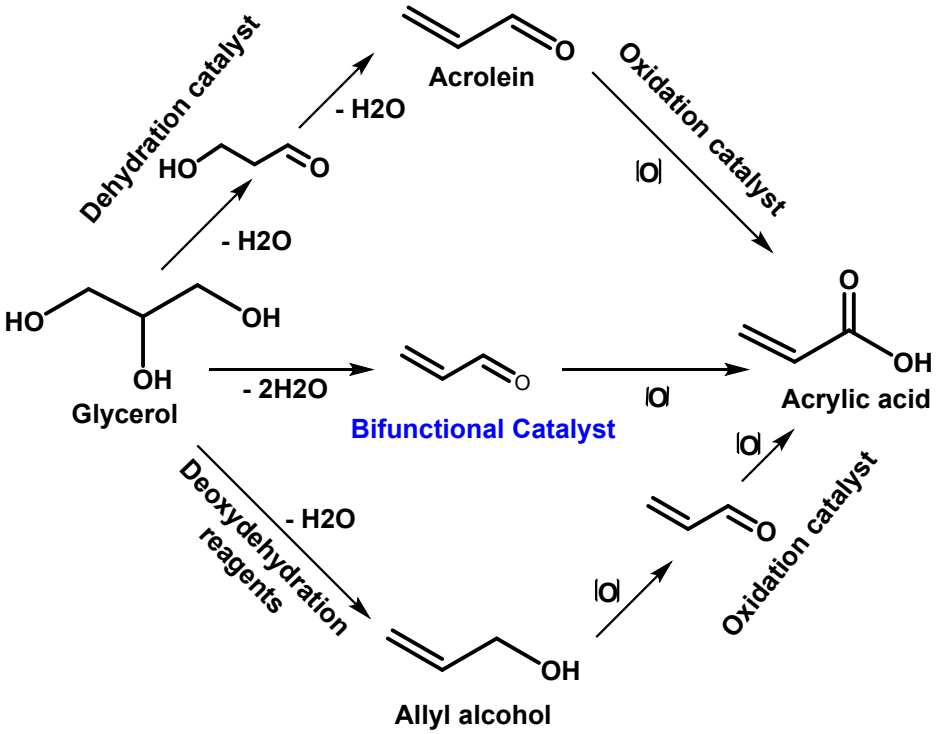

Scheme 2:

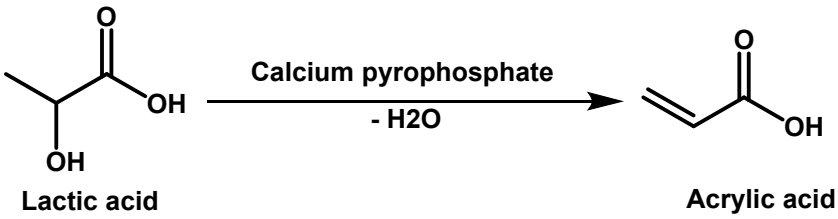

Scheme 3:

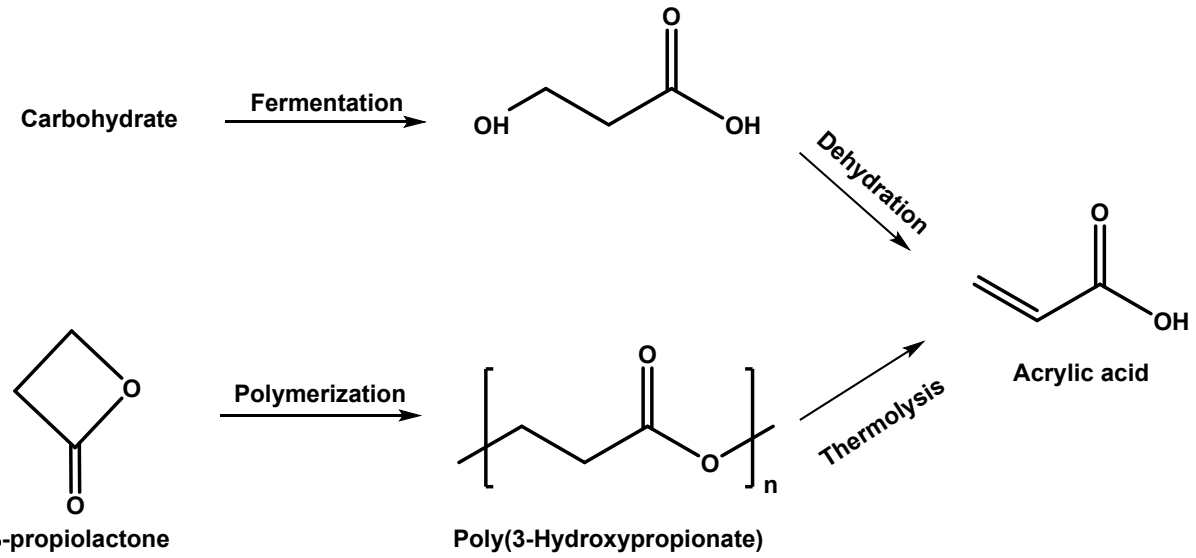

Scheme 4:

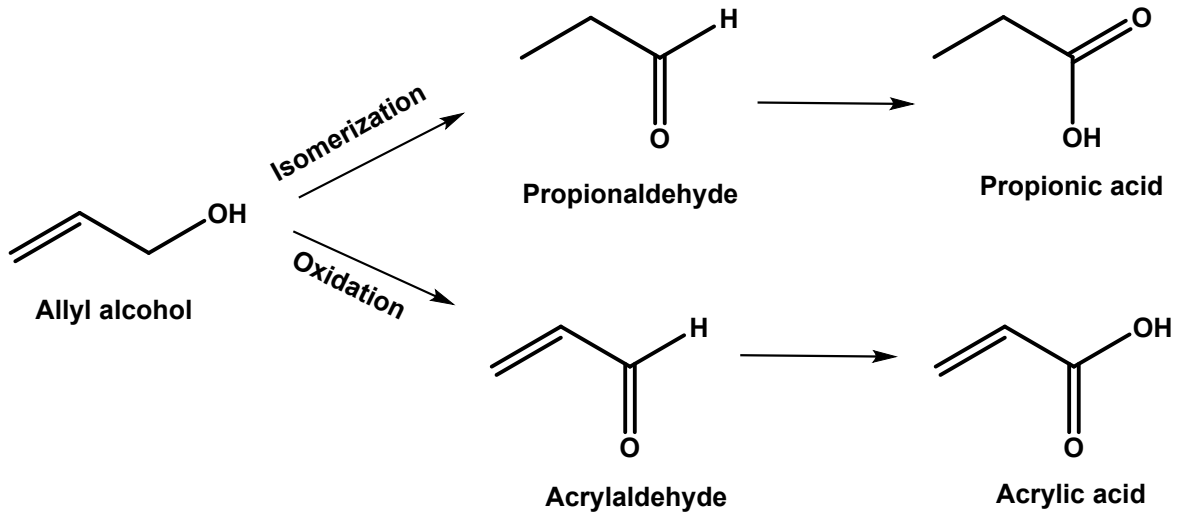

Scheme 5:

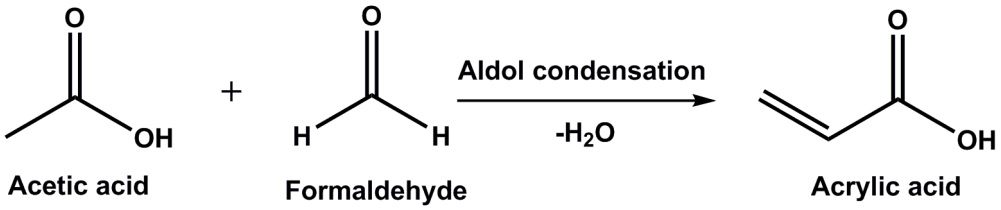

Scheme 6:

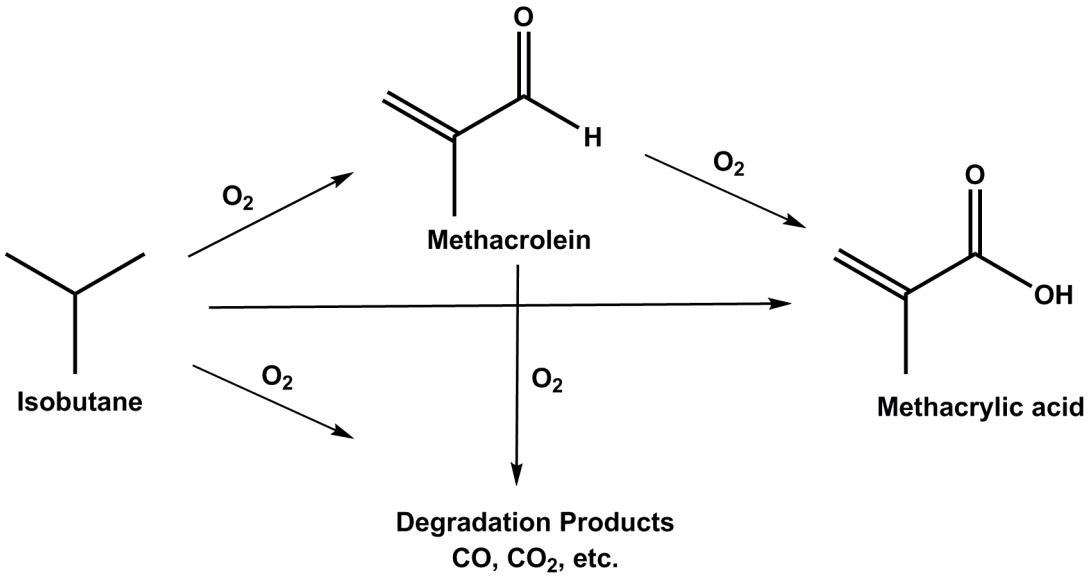

Scheme 7:

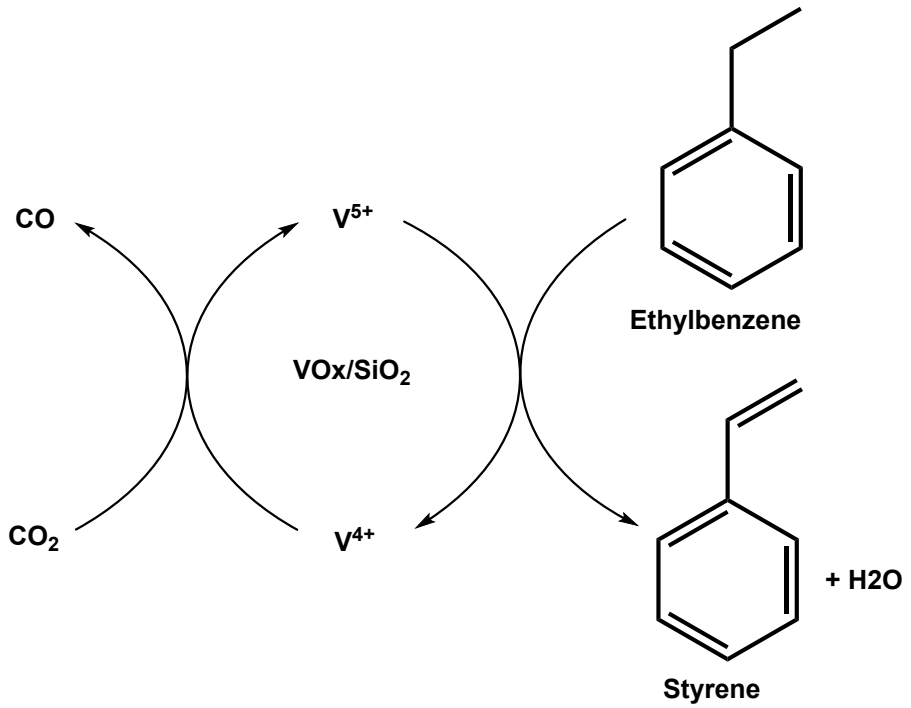

Table 1 Vapor-phase oxidative dehydration of glycerol to AA over heterogeneous catalysts.

Entry	Catalyst	Temp. (°C)	Conv. (%)	Sel. (%)	Ref.
1	W-V-Nb-O	300	100	34	42
2	FeVO	300	100	14	243
3	WVO	318	>99	26	244
4	WVNbO	265	100	50.5	245
5	MoVWO	290	100	42	246
6	MoVWO	250	100	30.5	247
7	H_3PO_4/WVNbO	285	100	59.2	43
8	$VH_3SiW_{12}O_{40}$/HZSM-5	90	100	36	45
9	$H_{0.1}Cs_{2.5}(VO)_{0.2}PW_{12}O_{40}$	340	100	60	46
10	VO/MFI-zeolite	350	100	17	48
11	Cu/SiO_2-MnO_2	70	77	74	49
12	Fe/HBEA-zeolite	275	100	23	50
13	H,Fe-MCM-22	320	93	57	51
14	HZSM-5/MoVO	250	100	47.2	247
15	HZSM-5/MoVO	300	100	40	251

Table 2. Oxidation of isobutane to MAA over $H_4PVMo_{11}O_{40}$-based catalysts.

Entry	Catalysts	Temp. (°C)	Conv. (%)	Sel. (%)	Ref.
1	$H_4PVMo_{11}O_{40}$	340	7	4	145
2	$H_3PMo_{12}O_{40}$(Py)	300	12	58	152
3	$Cs_{2.5}H_{0.5}PMo_{12}O_{40}$	340	16	24	154
4	$Cs_3PMo_{12}O_{40}$	340	7	12	155
5	$Cs_{2.85}H_{0.15}PMo_{12}O_{40}$	340	17	5	156
6	$(NH_4)_3PMo_{12}O_{40}$	352	5	42	157
7	$H_4PVMo_{11}O_{40}$	350	11	30	159
8	$Cs_{2.0}V_{0.3}PMo_{11}VO_{40}$	330	6	55	160
9	$Cs_{1.7}(NH_4)_{1.3}HPMo_{11}VO_{40}$	340	10	57	163
10	50APMV/$Cs_3PMo_{12}O_{40}$	340	14	47	162
11	$Fe_{0.85}H_{0.45}PMo_{12}O_{40}$	340	4	9	155
12	$Cs_2Fe_{0.1}H_{0.7}PMo_{12}O_{40}$	340	7	21	253
13	$Cs_2Fe_{0.2}H_{0.4}PMo_{12}O_{40}$	340	7	24	155
14	Cu-$Cs_{2.5}H_{1.5}$-$PVMo_{11}O_{40}$	350	18	3	169
15	$Cs_{2.0}V_{0.3}Cu_{0.2}PMo_{12}O_{40}$	350	13	47	170
16	$Cs_{2.0}V_{0.1}Cu_{0.2}PMo_{12}O_{40}$	350	14	30	170
17	$MoV_{0.3}Te_{0.25}$	390	15	12	172
18	$MoV_{0.3}Te_{0.23}Ce_{0.2}$	420	19	53	173

Table 3 Dehydration and decarboxylation of bio-based carboxylic acids into MAA over homogenous catalysts.

Entry	Catalysts	Substrates	Temp. (°C)	Conv. (%)	Yield (%)	Ref.
1	Hot compressed water	Citric acid	320	6	7	[175]
2	Hot compressed water	Itaconic acid	400	92	30	[175]
3	NaOH (0.2 M)	Itaconic acid	360	100	70	[175]
4	NaOH (0.5 M)	Itaconic acid	320	97	49	[176]
6	NaOH (0.5 M)	Mesaconic acid	320	100	52	[176]
7	NaOH (0.5 M)	Citraconic acid	320	98	40	[176]
5	NaOH (0.5 M)	Itaconic acid	250	55	19	[177]
8	NaOH (0.005 M)	Citramalic acid	250	80	34	[177]
9	NaOH (0.005 M)	Citramalic acid	300	100	81	[177]
10	Ruthenium carbonyl propionate	Itaconic acid	225	100	94	[178]

Table 4 Dehydration and decarboxylation of bio-based carboxylic acids into MAA over heterogeneous catalysts.

Entry	Catalysts	Substrates	Temp. (°C)	Conv. (%)	Sel. (%)	Ref.
1	Pd/C	Itaconic acid	250	89	47	179
2	$Pd(OH)_2/C$	Itaconic acid	250	94	57	179
3	$Pd/BaSO_4$	Itaconic acid	250	97	65	179
4	Pt/Al_2O_3	Itaconic acid	250	100	84	179
5	Pt/Al_2O_3	Citric acid	250	100	41	179
6	Pt/Al_2O_3	Aconitic acid	250	100	47	179
7	Hydrotalcite	2-HIBA	275	100	75	180
8	Hydrotalcite	Itaconic acid	250	25	23	180
9	Hydrotalcite	Citric acid	250	30	21	180
10	CHA	Itaconic acid	250	100	38	182
11	MHA	Itaconic acid	250	100	40	182
12	LHA	Itaconic acid	250	100	12	182
13	BHA	Itaconic acid	250	100	50	182
14	BHA	Citric acid	250	100	50	182
15	BHA	Aconitic acid	250	100	51	182

Table 5 Oxidative dehydrogenation of ethylbenzene to ST over vanadium based catalysts.

Entry	Catalysts	Promoters	Temp. (°C)	Conv. (%)	Sel. (%)	Ref.
1	$V/\gamma\text{-}Al_2O_3$	-	600	62	92	204
2	$V/\gamma\text{-}Al_2O_3$	-	550	52	97	203
3	$V_2O_5/TiO_2\text{-}Al_2O_3$	-	550	65	96	207
4	VO_x/HMS	-	600	74	99	202
5	$V/\gamma\text{-}Al_2O_3$	Cr	550	60	99	254
6	VO_x/SBA-15	La	600	80	94	255
7	V/activated carbon	Mg	530	62	99	256
8	VO_x/Al_2O_3	Sb	595	79	95	257
9	V_2O_5/Al_2O_3	Ce	600	65	96	258

Table 6 Oxidative dehydrogenation of ethylbenzene to ST over mixed oxide catalysts.

Entry	Catalysts	Temp. (°C)	Conv. (%)	Sel. (%)	Ref.
1	MnO_2-ZrO_2	650	73	98	210
2	K_2O/TiO_2-ZrO_2	660	65	99	211
3	Na-24/TiO_2-ZrO_2	600	72	97	196
4	MoO_3/TiO_2-Al_2O_3	650	77	97	261
5	$1.0Co_3O_4$/$MgAl_2O_4$	550	81	98	215
6	$Ce_{0.5}Zr_{0.5}O_2$	550	55	86	217
7	CeO_2/TiO_2-ZrO_2	600	74	98	218
8	CeO_2-ZrO_2/SBA-15	650	65	93	219
9	$Ce_{0.8}Fe_{0.2}O_2$	650	45	98	220
10	MAC-2	450	49	97	221
11	B_2O_3-Al_2O_3	475	46	94	223
12	TiO_2-ZrO_2/silicalite	600	<20	92	262
13	FeO_x-Al_2O_3	550	32	65	263
14	V_2O_5-CeO_2/TiO_2-ZrO_2	600	60	98	207

Table 7 Oxidative dehydrogenation of ethylbenzene to ST over carbon based catalysts.

Entry	Catalysts	Temp. (°C)	Conv. (%)	Sel. (%)	Ref.
1	AX-21	350	80	90	227
2	NT1	450	19	59	228
3	CNT700	500	50	65	229
4	UV/H35	400	47	91	232
5	BCN-800	500	54	89	233
6	ND/CNx-750	550	59	99	236
7	ND/CNF-FLG	575	39	93	237
8	ND	450	50	92	238
9	H-ND	550	56	99	239
10	N, O-ND/CNT-d	550	18	98	240
11	ND@NMC-0.02P/SiC	450	33	90	241

Table of Content

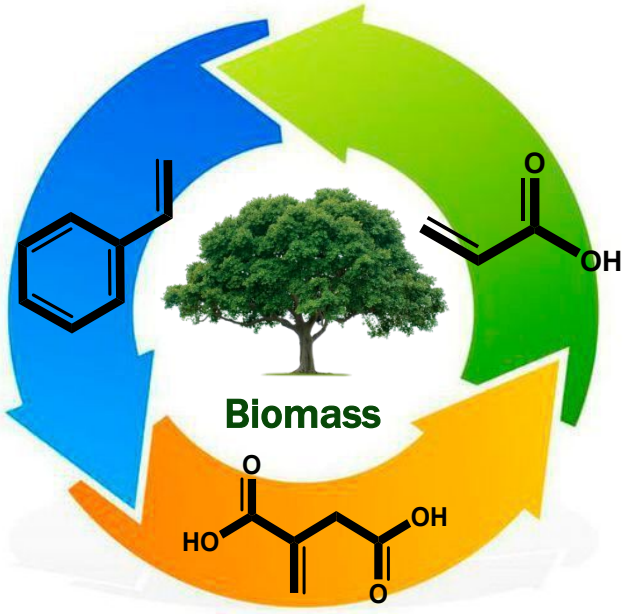

This review provides a summary and perspective for three bio-derived vinyl monomers – acrylic acid, methacrylic acid and styrene.